Development, Validation, and Application of a 3D print out of the Nasopharyngeal area from Cone Beam Computed Tomography in Children

by

Claudine Lopes Bussolaro

A thesis submitted in partial fulfillment of the requirements for the degree of

Master of Science

Medical Science - Dentistry

University of Alberta

ABSTRACT

Cone Beam Computed Tomography (CBCT) is increasingly being used in dentistry to explore certain types of craniofacial abnormalities. Sleep-disordered breathing represents a significant burden to individuals and society. Hence, the opportunistic use of CBCT imaging among dentists to screen for upper airway obstruction has increased. Adenoid hypertrophy (AH) is one of the abnormalities linked to upper airway (UAW) obstruction that could lead to obstructive sleep apnea (OSA). The specific use of CBCT imaging to assess AH and the related nasopharyngeal space has been already proposed, but there is still a lack of agreement on its diagnostic value. Dolphin software is widely used in North American offices due to its friendly-user capabilities. This software has an upper airway analysis function which could be used to generate an STL model of a specific upper airway section. To our knowledge, 3D print-out depictions of the nasopharyngeal area has not been explored yet. This thesis project aims to develop and validate 3D depictions of the nasopharynx including different degrees of AH. The 3D depictions (3D-picture and 3D-prototype) were produced based on a pool of CBCT scans of patients with the nasopharyngeal area already examined via Nasoendoscopy (NE). The design and development of the 3D depictions of pharyngeal adenoidal obstruction examples included two different representations of the nasopharyngeal airway, a lumen depiction (LU) and an adenoid mass in relation to the lumen depiction(AD). The developed methodology showed excellent reliability, ICC = 0.982 (95% CI, 0.939-0.995) for LU and ICC = 0.995 (95% CI, 0.981-0.998) for AD. The generated 3D volume surfaces (LU and AD) were converted into STL files and distinct types of prototypes were fabricated (LU 3D and AD 3D). Otolaryngologist-

head and neck surgeons (OHNS) evaluated the 3D depictions, the visualization consisted of LU and AD in 2D pictures and in 3D printed prototypes. Therefore four depictions were assessed in total, as follow: LU 2D depiction (surface picture), AD 2D depiction (surface picture), LU 3D depiction (prototype), AD 3D depiction (prototypes). One 3D depiction (LU 2D) failed to show validity as a subjective measurement; however, the other three 3D depictions (AD 2D, LU 3D, and AD 3D) were capable of suggesting validity as a subjective measurement. More precisely, the AD 3D depictions were adequate in detecting AH in this sample. High sensitivity and specificity were achieved 100% and 70%, as well as adequate positive predictive value (PPV) and negative predictive value (NPV) - 66% and 97% respectively. The developed 3D prototype may be a practical and readily available alternative for the assessment of the adenoidal obstructed area. It may also be useful in the future for educational purposes.

PREFACE

This thesis is an original work by Claudine Lopes Bussolaro. The research project was divided in four parts, that received research ethics approval from the University of Alberta Research Ethics board:

Project name “Development, Validation, and Application of a tool to Measure Pharyngeal Adenoidal Obstruction Level in Cone Beam Computed Tomography”, under number Pro00082445. No part of this thesis has been previously published.

ACKNOWLEDGMENTS

I would like to first acknowledge and express my gratitude to my supervisor and mentor Dr. Carlos Flores-Mir for his academic guidance, mentorship, pushing me to think critically and to strive for excellence. His patience and encouragement throughout my master program were imperative for my achievements. I want to thank my co-supervisor Dr. Camila Pachêco-Pereira and committee supervisor Dr. Manuel Lagravère for the many readings, editing, and invaluable feedback. I would like to thank the OHNS that agreed to participate in this project, especially Dr. Miguel Lerner, OHNS in Brazil, and Dr. Khal Ansari, Canadian OHNS, for their feedback on the prototypes. I would like to thank the technician Rishi Jaipaul for guidance and execution of the printer process, and Lara Pereira for performing the measurements for the inter-reliability process. I would like to thank the University of Alberta, the School of Dentistry for all the support, including awards and scholarships that supported me during this journey. I wish to acknowledge the director, coordinator and all the staff of the Faculty of Graduate Studies in the dentistry graduate program for their continuous dedication for making this program bigger and better, and aiming for worldwide recognition. I would like to thank all my friends cheering for my success, friends who offered their ears and shoulders to listen to me during all the disappointing and frustrating moments of this journey, and those who genuinely celebrate each of my great achievements. And lastly but not least, I would like to thank my parents, two visionary people, that even without higher education degrees were the first to plant the seed of the importance of education and to motivate in their daughters a mindset of “knowledge as a path for girl’s freedom and bright future”. I’d like to thank my family- my son, my daughter, my

husband, my sister, and my brother-in-law for their sacrifices, the cooperation, and for all the support I received for my dream to become real. My success in my graduate studies is a confirmation that behind every successful woman there is a tribe of other successful men and women who had had her back.

TABLE OF CONTENTS

LIST OF TABLES

LIST OF FIGURES

Chapter 1: Study justification and literature review on CBCT three-dimensional imaging use to assess upper airway

Chapter 2: Development of a 3d printed model of the nasopharyngeal adenoidal area using cbct

Chapter 3: Validation of the use of a 3D printed model depicting Adenoid Hypertrophy in comparisons to a Nasoendoscopy- based grading assessment

Chapter 4: Discussion & Conclusion

GLOSSARY OF TERMS:

2D	two-dimensional
3D	three-dimensional
A	ampere
ABS	acrylonitrile-butadiene-styrene
AD	adenoid tissue
AH	adenoid hypertrophy
ALARA	as low as reasonably achievable
BMI	body mass index
CAD/CAM	computer aided design/computer aided manufacturing
CBCT	cone beam computed tomography
CFD	computational fluid dynamics
CI	confidence interval
cm	centimeters
CT	computed tomography
DICOM	digital imaging and communications
ENT	ear, nose, and throat specialist
FNMM	fiber optic nasopharyngoscopy with Müller maneuver
HU	Hounsfield unit
ICC	intraclass correlation
LU	lumen
MCO	measured choanal obstruction space
MDCT	multiple detector computed tomography
MIT	Massachusetts Institute of Technology
mm	millimeters
MRI	magnetic resonance imaging

N	Newton
NE	nasal endoscopy, nasopharyngoscopy
NPV	negative predictive value
NS	non-significant
OHNS	otolaryngology-head and neck surgery specialists
OSA	obstructive sleep apnea syndrome
PLA	polylactic acid
PPV	positive predictive value
ROI	region of interest
SDB	sleep disorder breathing
SRDB	sleep related disorder breathing
STL	surface tessellation language
T	TESLA
UAW	upper airway
URS	upper airway resistance syndrome
UV	ultraviolet light
ηp2	partial eta-squared
μSv	microsieverts

Chapter 1: Study justification and Literature Review on CBCT three-dimensional imaging use to assess upper airway

INTRODUCTION

When a pediatric patient presents intermittent airway patency during sleep and the severity of this obstruction has not been evaluated through a polysomnography, this patient is said to have a syndrome of upper airway dysfunction during sleep, called obstructive sleep-disordered breathing (obstructive SDB).(1) Sleep disorder breathing (SDB) is characterized by a spectrum of clinical entities such as primary snoring, upper airway resistance syndrome, obstructive hypoventilation, and obstructive sleep apnea syndrome (OSA).(2)

The prevalence of OSA in the pediatric population is 1-5%(3), and the prevalence is even higher in children with comorbidities. Besides all individual deleterious effects, untreated OSA impacts the burden on society by increased health care costs, decreased work productivity, as well as motor vehicle accidents.(4, 5) The available literature reports that OSA costs around US$3.4 billion (USA), and US$ 7.4 million (Australia).(6) In addition, compared to age-matched controls, children with OSA consume six times more medication, need more specialist consultations and have a higher annual impact in health care costs, an increase of 215%.(7)

The first step in managing SDB in a pediatric patient is to assess a potential upper airway obstruction as the main cause.(1) The presence of hypertrophic adenoids has been quantified as the most likely cause of upper airway obstruction in children.(8) A recent systematic review(9) suggested a significant association between hypertrophic adenoids and upper airway obstruction as well as some links with specific dentofacial deformity traits. Hence, the assessment of the upper airway region is important in order to give any affected patient the management they need, preventing further major potential health consequences.

The clinical assessment of the upper airway region is usually comprised of direct clinical visualization, when possible, complimented by imaging exams which can be performed by functional, dynamic, or static techniques. Flexible nasopharyngoscopy (nasal endoscopy-NE) and magnetic resonance imaging (MRI) are the most common among the functional and dynamic imaging methods; computed tomography (CT), lateral neck radiography, and cephalometry are the most common among the static imaging techniques. In a recent consensus meeting of the European Respiratory Society task force on the diagnosis and management of SDB in children aged 2-18 years, it has been stated that all those exams and techniques could be used to evaluate abnormalities predisposing to obstructive SDB.(1)

In the medical field, the nasal endoscopy (NE) is considered the standard clinical visualization procedure used among otolaryngology-head and neck surgery specialists (OHNS) to visually assess sinus, nose, and any nasopharyngeal related pathology.(10) NE has some advantages such as radiation free and being a dynamic visual assessment but some disadvantages are also identified such as being a minimally invasive procedure that requires the development of determined technical skills. Its use is sometimes limited since during the exam the contact with sensitive structures can cause discomfort and pain to the patient. It is not considered a patient-friendly approach in children as it requires cooperation, occasionally sedation, and could lead to some level of complications.(10)

Considering that NE is out of the scope of practice for dentists, but that the overall assessment of the craniofacial structures is, the exploration of other imaging tools to assess the nasopharyngeal anatomy has been explored. Among them, CT and MRI can depict the morphology of the craniofacial structures; however, high ionizing radiation (specifically in the case of CT), limited availability, and associated costs, limit their day-to-day use.(11) On the other hand, CBCT is a relatively accurate and efficient modality involving less ionizing radiation than conventional CT.(12, 13) Hence, the use of CBCT scans in dentistry has exponentially increased since its introduction in the late 90's.(14)

The use of CBCT imaging and more specifically the accuracy and reliability of CBCT imaging contrasted against NE-based diagnosis for the assessment of adenoid hypertrophy (AH) has been previously reported in the literature in four studies.(13, 15-17) Excellent agreement between the two techniques (CBCT vs. NE) was found, although orthodontists, probably due to a lack of experience in CBCT, would make consistent errors in evaluating the 2D airway depictions from DICOM reconstructions. Thus, the use of a 3D printing model would benefit those professionals without experience with CBCT. The advent of a 2D and/or a 3D printed model could streamline the diagnostic process, especially in cases where the patients already had a recent CBCT in which hypertrophic adenoids is suggested. It would also substitute the need for an additional NE in selected cases and would be useful in remote regions where the access to an OHNS specialist is absent. It would also be used as a tool for patient education to increase awareness regarding the problem. Additionally, the exploration of 3D print outs of the nasopharyngeal area has not been explored yet and would be a good training tool to fill the previously reported(16) gap of agreement in image interpretation between professional assessments.

Besides its popularity in dentistry, the CBCT technique has the advantage of usually being more accepted by children in comparison to NE, as it causes neither pain nor major discomfort, and does not require sophisticated hand skills.(11, 18) Another advantage of CBCT over NE, is the fact that CBCT allows the use of a 3D software to convert the imaging in a 3D depiction which allows other anatomical areas to also be explored, enabling more applicability without a need for an additional exam.

Another reason to explore more applications for available CBCT DICOM's of the nasopharynx, is the current waiting time for patients to have the NE exam performed due to shortage of specialists (and staff) and, sometimes, inaccessibility. According to a paper published in 2016, 51% of Canadians wait extensively for a medical specialist appointment, and 53% waited too long for selected diagnostic tests.(19) The wait times for otolaryngology along with eleven other specialties has been considered the longest in the developed world.(20) The wait time has increased from 9.3 weeks in 1993 to 18.2 weeks in 2013, and has been implicated for the increasing rate of mortality in Canada.(20) The consequences of waiting may increase the rate of deterioration in general physical conditions, and also can lead to more complex medical interventions.

In addition, the health care environment is evolving and better integration and coordination between the dental and medical communities would benefit patient health(21). Patient health is the key concept of primary care, in which dentists sometimes are the active primary care provider, so that they can serve as a screening source for some chronic diseases, including OSA.(21) Dentists are responsible for the diagnosis, treatment, and prevention of diseases and disorders of the oral cavity and related structures.(21) Furthermore, dentists must fulfil the duty of care to the patient(22), and in the event of referrals, dentists should ensure the patient understands the importance of additional care. Hence, having dentists educated and trained in screening for SDB would allow them to provide proper referral to a medical specialist. Earlier diagnosis and treatment increases community health benefits.

3D printing is an advanced cutting-edge technology that has generated many applications in medicine and dentistry. It allows the rapid conversion of information from digital 3D models into physical objects. Surgical templates, diagnostic, rehabilitation, educational training, patient education and dental-medical records are some of the many possibilities.(10, 23-26)

For the above-listed reasons, we hypothesize that if CBCT is already available or indicated for other reasons, a 2D and/or a 3D print out of the nasopharynx may be capable of adequate discrimination between cases that likely have hypertrophic adenoids, which then should trigger selective referral to an OHNS. Furthermore, we want to compare the efficiency between both the 2D and 3D printouts in screening for adenoids.

1.1. Rationale

Five studies(13, 15-17, 27) have explored the use of CBCT to investigate pharyngeal adenoidal obstruction. Four(13, 15-17) contrasted with NE. Three(15-17) of them assessed qualitatively and one(13) quantitatively. Among the studies that assessed CBCT qualitatively, there is still some disagreement between professional image interpretation. In the quantitative assessment through volume and minimal cross-sectional area, a weak correlation was observed. In addition, the exploration of 3D printouts of the nasopharyngeal area has not been explored in this regard yet.

1.2. Study Importance and Justification

1. AH is associated with SDB in children:

Due to the individual and societal burden of SDB in children, over the years the literature has been reinforcing the need for early referral, diagnosis and treatment.

2. Dentist duty of care to the patient:

Dentists have the responsibility to screen for abnormalities on the stomatognathic system and craniofacial structures, and as a health care provider the dentist can serve as a screen for some chronic diseases, including SDB.

3. Wait lists in Canada:

Another reason to explore more applications for available CBCT DICOM's of the nasopharynx, is the current wait time for patients to have the NE exam performed due to a shortage of specialists (and staff) and, sometimes, inaccessibility.

4. CBCT imaging technology:

The advent of 3D printouts could enhance both the health professional's qualitatively and quantitative assessments of airway obstruction.

1.3. Objective

The objective of the present research is to develop and validate the use of 3D printed models of the nasopharyngeal area with different degrees of AH as a tool to screen for AH by OHNS assessments. (Figure 1)

1.4. Upper airway anatomy and function

Breathing is essential for human survival. Especially during childhood, this process is also of crucial importance for craniofacial growth and development. Normally breathing should occur almost exclusively through the nose, but when children cannot fully breathe through the nose, they will start to breathe through the mouth, which could facilitate undesirable adaptations of the stomatognathic system to an unusual role.(27-29) Additionally, pediatric OSA is often associated with a structural narrowing of the upper airway in conjunction with inadequate compensation for the decrease in neuromuscular tone.(30)

The upper airway consists of the pharynx, nasal cavity and surrounding sinuses. The pharynx is a 10.5 cm tube-like from the base of the skull to the lower border of the cricoid cartilage (C6) which sends air to the lungs, and food to the esophagus. The pharynx is usually divided into three parts: nasopharynx, oropharynx, and laryngopharynx.(31)

Those three parts of the pharynx have different functions. The nasopharynx has a respiratory function, the oropharynx has either a respiratory and a digestive function, whereas the laryngopharynx that communicates to the larynx, has a specific digestive function.(31)

The nasopharynx has its boundaries formed by five structures: the fornix (roof), soft palate (floor), choanae of the nasal cavity (anterior), mucosa covering superior constrictor muscle (posterior) and mucosa covering superior muscle (lateral).(31)

The anatomic features surrounding the nasopharynx are the ostium of the auditory tube, which opens into the nasopharynx; the torus tubarius lies superior to the ostium of the tube, the torus is an elevation formed by the base of the cartilaginous portion of the auditory tube; salpingopharyngeal fold is a mucous membrane that lies over the salpingopharyngeal muscle, connecting the torus tubarius to the lateral wall of the pharynx; pharyngeal recess is located posterior to the salpingopharyngeal fold, and contains the pharyngeal tonsils, also called adenoids.

In the nasopharyngeal space, we encounter the adenoids, a collection of lymphoepithelial tissues located near the oropharynx and nasopharynx, which was first noted in 1661 by Conrad Victor Schneider. He noted the adenoids between the vomer and the foramen magnum, being bounded by the pterygoid plates.(32) The adenoids' function was first considered to be a source of mucus, according to Schneider, and was not related to the speech or Eustachian tube function.(32)

In 1842, the improvement in hearing after removing this structure was reported by James Yearsley, but only in 1868, was Hans Wilhelm Meyer able to support the relationship between adenoids and ear disease and to develop an operation to remove the affected adenoids.(32) He successfully operated a 21-year-old patient who had hearing loss, difficulty speaking, dizziness, fever, otorrhea, and mouth breathing. Since then, removal of adenoids became rapidly accepted worldwide as a treatment for morbidities other than otitis, such as cognitive problems, speech problems, and sleep apnea; as well improvement of related knowledge and techniques have emerged.

More specifically, the adenoids compose the Waldeyer ring, a group of lymphoepithelial tissues, serving as secondary lymphoid organs, acting against antigens entering the body through the mouth and nose. Their size demonstrates age-dependent involution and appears to be correlated with the level of immunological activity, which peaks between the ages of three and ten.(2)

A link between hypertrophic adenoids and upper airway obstruction has been reported.(9, 33) Such obstruction may lead to SBD which in itself may lead to a compromised general health and quality of life.(8, 34) In addition, pediatric sleep disorders have been related to poor classroom grades, cognitive development, and attention disorders.(35)

1.5. Hypertrophic adenoids

The adenoids are exposed structures that are highly predisposed to inflammatory and infectious episodes, especially in children due to immaturity of the immune system.(2) In the first year of life, adenoids occupy a large part of the nasopharyngeal space, because of their role in immunity induction.(36)

They consist of 40% of T-lymphocytes, 50% - 60% of B-lymphocytes, and 3% of plasm cell, and they produce IgA.(36) Due to their anatomical location and immunological function adenoids are considered to be a reservoir of viruses and bacteria.(2)

According to Scammon's curve, which indicates the different pattern of growth on the human body, the lymphoid tissues start to decrease around 12 years of age(37). This pattern though cannot be applied to adenoid tissues because Scammon's curve did not evaluate tonsils and adenoids, but only the appendix, thymus, and intestine. Another exception of the Scammon's curve is the cranium-skeleton because the upper part of the face follows the neural curve and is completely grown around 7 years of age, while the lower face, follows the general curve having an adolescent growth spurt.(37, 38) The size of the adenoids vary, some children have enlarged adenoids since its birth, although usually the adenoids grow until 3-5 years old and start to diminish around the age of 7.(2, 36, 39) An age-dependent study conducted in 2013(39), concluded that adenoid sizes increase during the first 7-8 years of life, and then start to gradually decrease, and in snoring children the adenoids can remain large irrespective of age. AH in children has been associated with allergy and allergen(36), during the period the children are exposed to the antigens to which they are sensitized. So the period of enlargement varies depending on if it is functional, or reactional.(36)

1.5.1. Hypertrophy classification

AH can be classified based on many different methodologies, such as the Parikh, Wang, Fomin, and Cassano classifications.(40, 41) As demonstrated by a recent systematic review on adenoid prevalence, the Parikh(42) method was the most used method, followed by the Cassano classification.(41) The current reference standard is a subjective adenoid size grading scale system based on the relationship of the adenoids to the adjacent torus tubarius, vomer, and soft palate.(42)

1.6. Adenoid assessment in children

AH is a common disorder that can affect the efficacy of nasal breathing. If the adenoids become significantly enlarged, they can interfere with the airflow coming from the nose forcing the children to also breathe through the mouth, leading to undesirable adaptations. AH is the most common cause of upper airway space obstruction in children and adolescents, with a prevalence of 34.46% in randomized samples, and a prevalence ranging from 42.18 to 70.02% in a convenience sample.(41)

Various methods have been developed over the years for assessing adenoid sizes(8), mostly based on the available space in the nasopharynx around the adenoids, but not specific on the real size of the adenoid tissue. Palpation and mirror examination requires patient cooperation limiting the use in pediatric assessment.(11) NE is the primary method and the accepted reference standard to determine AH management(15), but it carries a level of inaccessibility and of some minimal risks such as laceration, bleeding, respiratory collapse, and vomiting.(18) Likewise, in patients unable to cooperate with the NE other imaging exams are considered.(11)

1.6.1. Nasoendoscopy

Regarding NE, the type of device to perform the procedure is not standardized as sometimes a rigid endoscope is used, sometimes a flexible one, and sometimes mobile units are used. Currently, flexible fiberoptic nasal endoscopy is a broad method used for multiple purposes in a routine OHNS practice.(8)

Fiber optic nasopharyngoscopy with Müller maneuver (FNMM) is used to assess the level of obstruction in the nasopharyngeal region while inspiration and expiration.(43) The technique is performed with the patient in a supine or sitting position, and with the endoscope in the nasopharynx the patient is asked to vigorously inhale with the mouth closed, while the examiner occludes the nostrils.(43)

1.7. CBCT

CBCT has been referred to as accurate in measuring facial soft tissue(44), and as an effective diagnostic method to evaluate upper airway space.(14) The use of CBCT to diagnosis AH has shown an agreement between CBCT and NE(15), and reconstructions of the adenoid tissue in 3D imaging, through CT techniques have been suggested.(45) Also, computer-based 3D volume calculations can be performed more accurately, effectively, and easily by the advent of 3D reconstruction and analysis techniques. A previous study concluded that orthodontists had poor agreement compared to NE to evaluate AH(16), therefore the advent of a 3D printout model as a part of dental documentation might improve nasopharyngeal obstruction assessment by general and specialist dentists, therefore facilitating the referral of the patient to a specialist.

1.7.1. Upper airway imaging

Imaging is one of the most important diagnostic tools in healthcare. Over the years a large number of imaging modalities have been developed based on different physical principles to visualize structure, function, and composition of the human body. Some of these imaging techniques are X-rays, nuclear magnetic resonance, ultrasound reflection, and radioisotope emission.(46) Within X-ray imaging different modalities such as conventional (film based) and digital such as computed tomography (conventional-CT, and electron beam CT-MDCT and

CBCT) have been used. Nowadays, computed tomography (CT), MRI, and cone-beam computed tomography (CBCT) are some of the most popular methods used in medical imaging.(47)

Medical history in addition to evaluation of clinical findings are the basis for the diagnosis of the upper airway dysfunction.(8) Functional, dynamic and static methods to evaluate upper airway have been described in the literature.

1.7.1.1. Functional Imaging

The functional imaging method includes the computational fluid dynamics (CFD) which assesses the airflow by computing analyses and simulation of the airflow. CFD is becoming a prominent technique, although it requires very specific abilities to perform and is time-consuming and computationally demanding.(48)

1.7.1.2. Dynamic Imaging

Dynamic methods include acoustic reflection, fluoroscopy, NE and nuclear MRI. Acoustic reflection is a non-invasive technique that allows the calculation of upper airway space volume as a function of the distance that the sound wave is reflected from/to its source. It does not involve radiation and can be repeated at 0.2 seconds intervals. A debated disadvantage is that this method does not provide anatomic information on discrete structures since the mouth remains open with a mouthpiece. Therefore, it may not compare well with other imaging techniques in which the mouth remains closed during the assessment.(12)

An alternative dynamic method, fluoroscopy has been used to assess airway closure during sleep, although radiation exposure makes the study impractical for routine use, and pertinent cross-sectional measurements of the airway are not possible.(12)

Nasopharyngoscopy also knowns as NE, is another dynamic method, that provides some advantages and disadvantages. Advantages include the fact that it can be performed either in supine or sitting positions, as well as either in wakefulness or sleep. Additionally, it allows performing the Müller maneuver, during the exam. The Müller maneuver can provide some insight into the location of the upper airways space obstruction by potentially mimicking obstructive apneas. As for disadvantages, it only assesses airway lumen and not surrounding craniofacial structures, and it is a relatively invasive procedure.

MRI allows both dynamic and static imaging(12), and it has excellent resolution for airways and soft and fat tissues, but it is costly and has limited availability. Images are displayed based on manipulation of nuclear magnetic dipole moments employing an externally applied magnetic field and subsequent recording and analysis of the radio signals emitted from the nuclei in response to these manipulations. The magnetic field measures in TESLA (*T*), one tesla is defined as the field which exerts a force of 1 Newton (N) on a one-meter length of a conductor carrying one Ampere (A) of a current perpendicular to the magnetic field.(46) Tesla relates to a gauss unit in that 1*T* is equivalent to 10,000 gauss. A whole-body MR scanner is voluminous and expensive and not necessarily needed for too many purposes; hence, smaller MR scanners have been developed, to accommodate limited field of views.

Due to the absence of radiation and the ability to make high-quality images of soft tissue(49), MRI might appear the most desirable for soft tissue and airway assessment, although the MRI exams take a long time to be completed, which might increase the probability of motion artifacts due to swallowing and movement; besides, it is not readily available for dentists.(30)

1.7.1.3. 3D Static Imaging

Amongst the static imaging, cross-sectional, volume, linear, and surface area measurements are included. The static method can also provide a 3D model, reconstructed from a 3D imaging modality.

CT is widely available, has an excellent airway space and bone resolution, and the structures can be viewed in 3D as well as in both dynamic and static methods. Using electron beam CT, some studies have analyzed in detail the airway changes during inspiration and expiration in wakefulness in normal and apneic patients.(50, 51) The drawback is that due to radiation it cannot be performed repeatedly during sleep and wakefulness.(12)

The interest in the role of CBCT, specifically the 3D imaging -static method- for treatment and outcomes in the upper airway space and craniofacial structures in patients with SRBD has grown exponentially.(48) Previously studies have suggested the use of CBCT to evaluate adenoids, tonsils and tongues(52), and upper airways.(14, 53) CBCT provided greater accuracy compared to MDCT.(54) MDCT provides high-resolution images but has radiation doses around 860 μSv for a 12-cm-high field of view.(55) Additionally, it is not readily available for dentists. On the other hand, CBCT has ten times less ionization radiation, around 68 μSv(56) and is readily available for dentists.(48) Additionally, CBCT cost is lower than the other two (CT and MRI) and has high clinical application in the field of dentistry.

1.7.2. CBCT imaging formatting before visualization

The difference between CBCT and a conventional CT is that CBCT uses a cone-shaped beam that captures the full image in a single rotation. So, the patient should not move during the exam. Technically, it is a squared matrix of pixels (picture elements), each representing a voxel, in a slice of the region of interest. The series of measurements collected by the CT scanner are assigned a gray value based on the magnitude of contrast. Slightly attenuating structures like air are shown in black, and the highly attenuating structures like compact bone are shown in white.(46)

For image reveal, each pixel is appointed a CT number representing tissue density, this number is named after its creator Sir Godfrey Hounsfield.(57) Hounsfield unit scale (HU) refers to the linear transformation of the original linear attenuation coefficient value of each tissue, and it measures radiodensity on a quantitative scale.(49, 57-59) Although, HU values for CT machine was first defined as -1000 HU for air while distilled water were defined as 0 HU(57-59), HU is not an absolute value and can change based on imaging parameters and CT scanners.(49, 60) For instance, the initial HU values were represented from -1000 to +1000(57), while newer CT machines have a range up to 4000 HU.(49) Another important observation is that many tissues differ by only few HU, therefore only if a small range of HU is displayed those tissues can be differentiated.

In CBCT, the degree of x-ray attenuation coefficient is shown by gray scale values instead of HU scale, even though some CBCT manufacturers and software present the gray scales named as “HU”, note that this HU CBCT terminology does not hold the same value as the actual HU CT. Basically, “gray scale” and “HU” do not share the same value and scale until now. Still, a number of studies(59, 61-67) have observed the relationship between HU values and gray scale for bone tissue density (59, 64-67), with generally consistent findings, although under distinct scan protocols. Nevertheless, while bone density values correlation between HU CT and CBCT gray values has been widely explored, the opposite can be said regarding literature about the correlation in values for air and soft tissue. Air indeed, showed a great difference between grey levels and HU values being excluded from the curve fit.(65)

In CBCT, an image with low density (considered radiolucent in 2D radiographs) is called hypodense and with high density is called hyperdensis. Voxels with a number below than the upper limit will be displayed in black and higher than it will be in white.(46) Due to this imaging principle, the dimensions of a structure may be distorted in regions where different tissues meet, for instance between soft tissue and bone as the boundary may not be clearly differentiated.(46) This distortion becomes more pronounced the thicker the sections are because more different tissue's density will be in the same voxels.(46)

1.8. CBCT and 3D reconstruction use to assess upper airway space and surrounded structures

The 3D imaging reconstruction tool has been positive for complex medical cases as it significantly improves diagnosis and treatment planning. The use of the digital imaging and communications in medicine (DICOM) format allows the 3D reconstructions of complex airway space and anatomy.(29) As a result, new possibilities and applications for CBCT in upper airway imaging analysis have become increasingly relevant.

Since dentists might be among the first professionals to recognize a patient's potential sleep-breathing problem(68, 69), SRBD has become an area of interest in dentistry. Consequently, general dentists and specialists have become more familiar with screening tools for potential nasal airflow reduction or obstruction, of which AH is a chief cause.(70)

A previous study evaluated the airway volume and minimal cross-sectional airway area from a CBCT against the NE using an automated tool of Dolphin software to localize the constricted area. They concluded that the automated measurements may not yield high quality clinically relevant information on the upper airway constriction related to AH.(13) Nonetheless, their methodology presented some limitations regarding delimitation of the region of interest that overly delimited the adenoid anatomic limits area. Another important limitation is that they included patients in their sample that did not have the CBCT and NE performed on the same day. Thus, their results would be compromised both for the measurements, as well as for the variance in the level of adenoid obstruction due to the NE diagnostic and CBCT exam dates. Therefore, there is a need for the exploration of 3D printing as an alternative to overcome the disparities in diagnosing from ENTS on CBCT.

1.9. 3D printing

Prototyping technology and 3D printing was introduced in the 1980s, and just recently made some impact on the research and medical industries.(71) The 3D printing technology works through a 3D model file, which is imported into a program called a “slicer”. The program slices the “object” into single layers and creates a code that informs the printer regarding movements, speed, and temperature. The object is then manufactured by laying down successive layers of material until the 3D object is complete. It works by joining, bonding, sintering or polymerizing small volume elements, producing a solid object from a digital file.

3D printing is a cutting-edge advanced technology that has generated many applications in the medical and dentistry fields. It allows the rapid conversion of information from digital 3D models into physical objects. Surgical templates, diagnostic tools, rehabilitation, educational training, and diagnosis are some of the many possibilities.(10, 23) The ability to plan and perform surgery on a 3D printed model beforehand as a simulation of the actual procedure has been impressive.

1.9.1. Principles of 3D printing

Some of the 3D printing technologies in dentistry include laser, fused deposition modeling, digital light processing, and stereolithography (SLA).(23) Selective laser melting makes metallic frameworks, using heat generated by computer-controlled laser radiation. In the fuse deposition modeling a scan informs the printer to deposit melted thermoplastic polycarbonate, the resulting aspect of the object can be used in combination with acrylic or wax. In the digital light processing, the object is built on an elevated platform and with information coming from a projector light-curing a liquid resin layer by layer. SLA is the most popular rapid prototyping technology which principle is based on a photosensitive monomer resin. It forms a polymer that solidifies when exposed to ultraviolet (UV) light.

SLA printing was invented in the 1980's and became more popular through prototyping in the 21st century. In 1983 Charles Hull printed a 3D object using a 3D printer, back then its use was more popular in the architecture, aeronautics, and telecommunications sectors.(72) In 1986, he founded 3D systems and developed the first commercial 3D printing machine, stereolithography Apparatus. In 1993, the 3D printing technique was patented by the Massachusetts Institute of Technology (MIT).(73) In the 1990s, it was implemented in the medical field due to the millimetric precision.(72)

1.10. From CBCT DICOM to STL - Image acquisition and Post-Processing form

The 3D printing technique involves data acquisition, processing and the fabrication using additives.(23) The first requires images obtained from a CBCT converted to a Surface Tessellation Language (STL), also called "standard triangulation language" file. It is a file format native to the stereolithography CAD software created by 3D systems, and this procedure is called photo-polymerization. This type of technology is considered the most accurate form of 3D printing. Glass-filled polyamide, silver, steel, titanium, photopolymers, wax, polycarbonate, stereolithography materials (epoxy resins), polyamide(nylon), polylactic acid (PLA) and acrylonitrile-butadiene-styrene (ABS) plastic are some of the materials used for printing.(23)

1.11. 3D in Dentistry

Over the past 30 years, prototyping and 3D printing have been providing better quality and comfort for dentists.(72) In maxillofacial prosthesis, prosthodontics and restorative dentistry, prototyping promotes faster production and better quality outcomes compared to conventional dental technicians. In oral surgery and implantology prototyping helps to minimize risks that might occur during the surgery.(72)

In dentistry, the 3D printing technology has been explored from DICOM images and CAD/CAM Scanners; bioprinting is still in its initial research exploration in the dental field. The most common use of 3D printing in dentistry is by oral scanners, which are used for dental restoration, prostheses, implant restorations, dentures, orthodontic appliances, and to print craniofacial structures for reference before complex surgeries, and forensic applications.(73, 74)

To assess the literature regarding 3D printing from CBCT 3D imaging, we performed a literature search using the words “3D printing” and “dentistry” on Medline, on January 2, 2019, and 248 papers were found. Among them, only 35 articles with CBCT application were found. Some of them were excluded from our analysis because of study design – review, systematic review, or not being a human study, or not evaluating 3D printing models originated from a CBCT. After reading the titles and abstracts, only 14 met our selection criteria. Among all, four (75-78) were in the endodontics field, in which two(76, 77) of them were exclusively for educational purposes. Four(79-83) were used for prosthetics rehabilitation, among them three (80-82) were used for maxillofacial prosthesis, and one(79) in oral prosthesis. Six were in the oral maxillofacial surgery field(84-88), among them one(85) was in implantology, one(86) in periodontology, and one in orthodontics(88). Table 1.1 shows the results of the literature search.

Regarding upper airway CBCT-3D printing, in 2012, a study(89) created a prototype of the oropharynx using MIMICS software, and from that evaluated the sensitivity threshold using Dolphin software. A recent study(90) printed the oropharynx space and compared the accuracy between MDCT and CBCT. Two MDCT scanners and three CBCT scanners were used, and the volume and cross-sectional areas were measured. The measurements were analyzed against a 3D-printed anthropomorphic phantom of the oropharynx from a real patient CBCT data set, which was determined as a gold standard phantom. They concluded` that CBCT scanners offer an alternative to MDCT in the assessment of the oropharynx morphology. Nonetheless, the assessment of a 3D printed model from CBCT as a computational aid for screening for abnormalities and obstruction diagnosis of the nasopharynx has not been explored.

The 3D printing is a technology that converts a 2D image to a touchable 3D model, enabling a more comprehensive study of human anatomical structures, especially complex anatomies. Even for dentists it is a challenge to identify some alterations in the nasopharyngeal space, therefore, it must be even more difficult for a layperson who doesn't know anatomy. As

3D printed models are capable of providing tactile feedback and actual depth information about anatomic and pathologic cases, it would work as an aid to educate and raise awareness in affected patients and especially their parents about the importance of looking for a specialist. (26)

In conclusion, few studies have explored the use of CBCT for 3D printing in dentistry, additional the use of CBCT 3D printing as a computational aid for screening diagnosis needs to be explored further.

1.12. Clinical significance

Dentists probably see their patients more frequently than physicians, and hence are often among the first line of detection of health issues.(91) The consequences of AH in children go from craniofacial deformities to obstructive sleep apnea, which can lead to more serious disease as pulmonary affections, cardiac, and even death in sleep in younger children.(92)

The influence of AH in the deformity in the dental arc and facial skeleton, due to mouth breathing has been explored. When children cannot breathe through the nose, they unconsciously start breathing through the mouth, this process leads children to develop specific shape in the face, called “adenoid face”.(93) Characterized by an increased anterior face height, an increased mandibular plane angle, a narrow and high maxillary arch, a retro positioned hyoid bone. Due to facilitation on nasal breathing, improvement in mandibular growth and closure of the mandibular plane angle have been reported after adenoidectomies.(93) Increase in school performance also correlated to post adenoidectomies. (94, 95)

A call for leadership in dentistry regarding child health care, and the need for interaction between the dentist and medicine for the child’s good, and a need for partnership at all levels of society to promote oral health and prevent disease has been addressed.(96) Also, an emphasis on the need for dental-medical education collaborations intended to decrease oral health disparities.(96)

Dentists may play an essential role in screening and referring potential patients with risk factors for SRDB since evaluation of the oral cavity, as a patency of the airway and neck circumference, so it is essential that general practitioners are educated and trained regarding SDB, so they can work closely with a referral system to the proper specialist for diagnosis and treatment.(91)

1.13. Hypothesis

The first objective of this study is to develop a reliable methodology to build 3D depictions of the nasopharynx depicting the adenoidal region.

First hypothesis:

H_o= CBCT methodology for the development of 3D depiction tools of the nasopharyngeal adenoidal area is not reliable.

H_a= CBCT methodology for the development of 3D depiction tools of the nasopharyngeal adenoidal area is reliable.

The second objective of this study is to validate 3D depiction tools of the nasopharynx depicting adenoidal region for screening for AH.

Second hypothesis:

H_o= 3D depiction tools of the nasopharyngeal adenoidal area are not accurate in screening for adenoid hypertrophy compared to the NE diagnosis made by an OHNS.

H_a= 3D depictions of the nasopharyngeal adenoidal area are accurate in screening for adenoid hypertrophy compared to the NE diagnosis made by an OHNS.

1.14. Figures & Tables

Figure 1. 1– Project process map

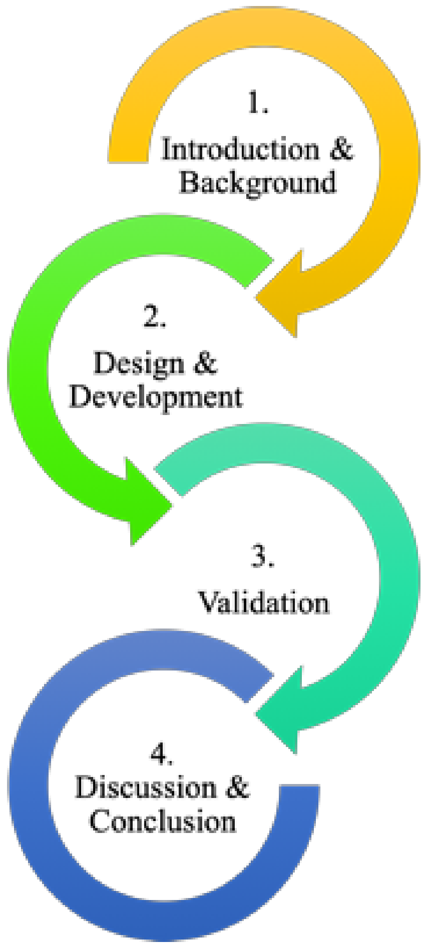

Table 1. 1 Literature search on 3D printing in dentistry

Author	Year	Country	3D printing	Clinical Field	Educational Field
Ahn, SY et al.	2018	USA/South Korea	Surgical template	Endodontics	
De Souza, N et al.	2018	India	Surgical template	Oral Maxillofacial Surgery	
Lin et al.	2017		Removable dental prothesis	Prothesis	
Ma B et al.	2018	Republic of Korea	Surgical guide	Implants	
Martinez-Seijas P et al.	2018	Spain	Orbital Prosthetic	Maxillofacial Prosthesis	
Murat S et al.	2018		Hemi-maxilla resin mold	Maxillofacial Prosthesis	
Nuseir A et al.	2018	Jordan/UK/Saudi Arabia/Egypt	Nasal reconstruction	Maxillofacial Prosthesis	
Reymus M et al.	2018	Germany	Hands-on training course	eriodontology (dental trauma)	Student education
Reymus M et al.	2019		Root canal treatment training	Endodontics	
Van der Meer et al.	2016	London/Nettherlands	Digital endodontic treatment planning	Endodontics	
Verweij JP et al.	2017	Netherlands	Tooth Template Guide/autotransplantation	Oral Maxillofacial Surgery	
Wang YT et al.	2017	Taiwan	Miniscrew using surgical templates	Orthodontics/Oral surgery	
Yahata Y et al.	2017	USA/Japan	Research in 2 different endodontic treatment tecnique	Endodontics	
Ye S et al.	2018	China	Surgical planning, surgical template	Oral Maxillofacial Surgery	
Alves, M et al.	2012	Brazil	Is the airway volume being coorrectly analyzed?	Orthodontics	Reliability Research
Chen e t al.	2018	Netherlands	Accuracy of MDCT and CBCT in three-dimensional evaluation of the oropharynx morphology	Orthodontics	

Published literature on 3D printing of the AIRWAY					
Author	Year	Country	Title	Clinical Field	Research Field
Alves, M et al.	2012	Brazil	Is the airway volume being coorrectly analyzed?	Orthodontics	Research
Chen e t al.	2018	Netherlands	Accuracy of MDCT and CBCT in three-dimensional evaluation of the oropharynx morphology	Orthodontics	

Chapter 2: Development of a 3D printed model of the nasopharyngeal adenoidal area using CBCT

INTRODUCTION

Partial or complete nasopharyngeal obstruction compromises an essential physiologic mechanism for humans to survive that is the breathing process. Breathing is also of significant importance to children's craniofacial development and growth. Under normal conditions, one should breathe exclusively through the nose; when children cannot breathe enough air through the nose they start complementing their breathing intake by using the oral cavity. If this is chronic it may promote undesirable adaptations by the stomatognathic structures.(27-29) These breathing adaptations could alter deglutition, speech and mastication, ultimately leading to alterations in craniofacial growth and development.(97, 98)

Back in 1661 adenoid hypertrophy (AH) was linked for the first time to speech problems, otitis, sleep apnea and cognitive problems.(32) Adenoids are a collection of lymphoepithelial tissues located near the oropharynx and nasopharynx. If adenoids become enlarged, they can interfere with airflow coming from the nasal structures to the lungs forcing children to also breathe through the mouth, which may lead to functional and/or anatomical adaptations.

AH is the most common cause of upper airway obstruction in children, with a prevalence ranging from 34% to 70% accordingly to a recent meta-analysis.(41) A recent systematic review suggested a close association between hypertrophic adenoids and upper airway obstruction.(9) Distinct studies(1, 8, 34, 98) have linked AH to Sleep Disordered Breathing (SDB). SDB can have major negative effects in general health and quality of life. In addition, pediatric sleep disorders have been related to poor classroom performance.(99) Thus, in order to prevent craniofacial, overall health and behavioral alterations, an early AH diagnosis by a pediatric otolaryngology-head and neck surgery specialist (OHNS) is highly desirable.

Medical history (signs and symptoms) and physical examination combined to an objective exam is paramount for a precise upper airway obstruction diagnosis.(1, 70, 100, 101) NE is the frequent chosen office procedure to assess sinus passage, nasal, and any nasopharyngeal related pathology by OHNS.(10, 42, 100, 102) Studies by Chisholm et al. and Zalzal et al.(103, 104) have cited Kubba et al., 2001 as first referring to NE as the “gold standard”. Nonetheless Kubba et al. 2001, did not state that; additionally, his study was performed under general anesthesia, which does not reflect the real scenario of a routine NE in most of the ENTs office.(105) NE under topic anesthesia, can be a distressing procedure for young children, NE could cause discomfort and pain to the patient, and needs cooperation in young children.(103-106) Besides the popularity of NE, radiographic images have been referred as better planning tools and are also important for diagnosis.(107) To date, there is no comprehensive guideline for assessing adenoidal enlargement in children.(100)

Lately attempts have been made to explore the use of CBCT imaging to assess the nasopharynx for screening purposes. CBCT imaging does not cause pain or discomfort, is less physically invasive, does not require sophisticated hand skills, and is usually more accepted by children when compared to NE. The main problem with using CBCT is the additional ionizing radiation exposure. CBCT has the potential to provide a 3D reconstruction of the nasopharynx and permit the assessment of potential HA obstruction. It is important to make it clear that the intention is not to request a CBCT for nasopharyngeal assessment but the fact that such craniofacial imaging could be readily available for other reasons and also be used for upper airway assessment.

Three-dimensional (3D) printing is a cutting-edge technology which has been increasingly used in medicine and dentistry.(72) The exploration of 3D printouts of the nasopharyngeal area has not been investigated yet. The goal of this chapter was to present reliability of the process to generate a 3D printed model of the nasopharyngeal area with distinct degrees of AH.

2.1. MATERIAL AND METHODS:

The Research Ethics Committee at the University of Alberta approved the protocol number Pro00082445 for the present cross-sectional reliability study.

This study followed the ALARA principle (As Low As Reasonably Achievable) by the European Society of Radiology, thus, CBCTs were not specifically taken for this study. All imaging was pre-existing and were taken using the ICat scan (Classic, Cone Beam 3D Dental Imaging System; Imaging Sciences International, Hatfield, Pa). These were taken by using 6.19 mAs, at 110 kV, and with a customized height field of view maximum of 12 in, 0.3 mm voxel, and 8.9-second scan time with the patient in an upright position at maximum intercuspation. The DICOM data was analyzed using an automated reconstruction commercial software (Dolphin 3D, version 11.95 premium, Dolphin imaging & management Solutions, Chatsworth, CA, USA)

A list of 40 patients assessed at the Orthodontic Graduate Program and the Inter-disciplinary Airway Research Clinic at the University of Alberta. Inclusion criteria included having both a CBCT and NE assessment of the nasopharyngeal area done at the same day. Exclusion criteria included (1) scans in which the defined airway volume was not clear or fully contained in the image; (2) patients that had previous adenoid surgery, and (3) patients whose records did not have a clear description of the adenoid assessment through NE by the ENT, and (4) patients that did not have the CBCT performed on the same day as the NE. (Flowchart A)

For reliability purposes a sample of 12 CBCT - 3 subjects for each adenoid graded size(42) were randomly selected from the total sample. Two evaluators were previously calibrated using 4 randomly selected CBCT's.

In order to standardize the assessment of the images a skull orientation was established as follows:

In the frontal view: (Figure 2.1A)

- **Axial plane**: determined at the level of anterior nasal spine
- **Mid-sagittal plane:** determined at the anterior nasal spine.

In the right view:

- Determined at the **coronal plane** oriented at the lateral orbital border at first. (Figure 2.1B)
- **Coronal slice (green line):** this second calibration was done right before the delimitation of the area of the interest. This second calibration was defined at the level of posterior nasal spine as seen in figure 2.1C.

The superimposition of the lower right and left mandible borders was checked, in the right view; as well as adjustments were made to rotate the volume clockwise, side-to-side, and up/down until the edges were as most coincident as possible. Then the left view was checked for any adjustment.

Bottom (facing up), and top (facing down) were also checked all at once for any additional orientation adjustment. Figure 2.1D shows the orientation plane in 3D view.

2.2. Design and Fabrication

2.2.1. Methodology for airway assessment (Lumen-LU) (Figure 2.2 to 2.4)

The delimitation of the nasopharyngeal area of interest was made on the sagittal and axial anatomical planes. We modified one previously developed method(108) used to measure the nasopharyngeal airway volume. The landmarks were selected based on the anatomical location of the adenoid gland, The Sinus/Airway tool in Dolphin software was used to select the landmarks as explained below:

- **Sagittal plane:** *sella turcica*, anterior tubercle of the atlas bone (C1), tip of the uvula and posterior nasal spine.
- **Axial plane:** posterior wall of maxillary sinus; right and left anterior point of cervical vertebrae, at the level of the most anterior point of the Atlas.

A seed point was placed in the airway space so that the software could capture the designated airway surface. The sensitivity tool from the semi-automated software was adjusted to 35, which was the value that better depicted the empty region (air) in our sample.

Figure 2.2 shows the landmarks in sagittal view (A) and axial view (B) as well as the seed point and the airway surface in yellow. Figure 2.3 shows a representation of the lumen (LU) surface in the translucent hard tissue view. Table 2.1 shows an example of the 3D LU volume surface representation (yellow) in bottom, top, front and right view for each one of the four different grades, depending on the level of adenoidal obstruction on the nasopharyngeal space. The grading ranges from 0 to almost complete obstruction. grade 1, when the obstruction is from 0-25%; grade 2, >25%-50%; grade 3, >50%-75%, and grade 4, > 75%.(42, 109)

Table 2.2 shows the anatomical representation of the localization of region of interest (ROI) represented by the superimposition of the 3D LU surface within the hard tissue.

A schematic representation of the anatomical limits of the LU volume surface is shown in Figure 2.4.

2.2.2. Methodology for AD assessment

For the adenoid assessment, the same orientation previously defined was followed, and the ROI was stablished on the following landmarks that was based on the modification of two previously used methods.(17, 108)

Sagittal landmarks:

- Most inferior image of occipital bone;
- Most anterior point in spheno-occipital synchondrosis;
- Intersection point between palatal bone, and uvula anterior wall;
- Tip of uvula;

Axial landmarks were stablished at the level of Atlas:

- Most posterior wall of R and L maxillae (R and L paranasal sinus).
- two lateral R and L landmarks at the Atlas, at the level of the anterior tubercle

Two seed points were placed over the adenoid and the uvula, and the HU were set to -561 for the lower bound, and 3250 for the upper bound for all cases but one case in which the upper bound adjustment was not possible at 3250 and had to be set at 3052.

Delimitation of the region of interest (ROI) with the landmarks for the surrounding soft tissue (adenoid and soft palate) is shown in Figure 2.5. Table 2.3 shows the representation of the

AD, and table 2.4 shows the anatomical representation of the localization of region of interest (ROI represented by the superimposition of the 3D AD volume surface within the hard tissue.

Figure 2.6 shows a schematic representation of the surrounding anatomical structures. Figure 2.7 shows the superimposition of the two models

2.2.3. 3D printed model process

Both created volume surfaces that were saved into STL file and sent to the Centre for Teaching and Learning laboratory, at the University of Alberta.

The Afinia H800 3D printer (Chanhassen, MN, USA) (Figure 2.8) fabricated the models by uploading a file including the 3D image to its software, Afinia Studio software via USB to a HP laptop. Once uploaded on the software the size of the print was not changed to maintain the actual size of the anatomical structures. The printer used premium acrylonitrile-butadiene-styrene (ABS) filaments. The color of the filament was chosen as follows: yellow for the LU model, and red for the AD models. The filaments were loaded into the filament spool on the printer. For the adenoid models the printer used approximately 15 grams of ABS for each model; for the airway space model it used approximately 5.3 grams of ABS each.

The actual models created by the printer reproduced exactly the 3D surface generated by Dolphin software as seen in Figure 2.9. Figure 2.9 shows the 28 prototypes - representing grade1, grade2, grade 3 and grade 4.

2.3. Statistical Analysis

The intra-class correlation coefficient (ICC) was used to assess intra and inter-reliability of both evaluators (CTB and LPP). Descriptive analysis of all data including means, standard deviation, minimum and maximum values were determined using the Statistical Package for the Social Science (IBM, version 25; SPSS Inc., Armonk, NY, USA). The level of significance and confidence interval (CI) was set at 0.05.

2.4. RESULTS

As the calibration result, ICC was used to analyze the reliability. A high intra reliability was found for both types of models. For UA models an ICC =0.993 (95% CI:0.981-0.998) and for AD model an ICC =0.944 (95% CI: 0.861-0.982) in single measures, were found. Inter reliability was considered excellent between raters for both models; LU presented an ICC of 0.982; 95% CI, 0.939-0.995); and AD presented an ICC of 0.995; 95% CI, 0.981-0.998). Sample demographics and measurement Information can be seen in table 2.5

The volume measurements were assessed at three different times with three days washout period. A different spreadsheet was used between the measurements to secure blindness. The measurement error for LU was 1.667mm^3 ± 1.000 mm^3 (SD: 37.27 mm^3), and for AD was 139.250mm^3±1.006mm^3 (SD: 98.46 mm^3).

2.5. DISCUSSION

This chapter refers to the second part of the present research project, which involves the design and development of the two 3D printed models. Reliability of the methodology was the key consideration in this design process. The intra-rater and the interrater reliability were confirmed by the ICC, and high reliability was found for both assessments.

The prototypes were developed using the DICOM data analyzed with commercial software Dolphin 3D. A previous study(89) had reconstructed an oropharynx airway with

Mimics software, and a later study had compared both softwares, Dolphin and Mimics, and both showed less than 2% errors on volume measurement. We chose Dolphin software because it is considered the most commercial software used in maxillofacial surgery and in the orthodontics field in the north America, and the software has shown high reliability for airway measurement in previous studies.(89, 110) Moreover, Dolphin software allows the created surface to be saved in an STL file, so we don’t need additional software for that purpose. Nonetheless, the same methodology could be applied to another software to verify its 3D printing feasibility.

Older versions of the software only allowed the measurement of the volume of empty areas(89), but the latest version of the software (11.95), the one we used on our study, allows for the measurement of the volume of tissues and bones due to an inverted threshold tool. As far as we know, our study is the first to report the technique of using the inverted tool, and to test the feasibility of the software in converting the surface to an STL file, as well as to generate a 3D printed prototype based on that.

In our study, we excluded cases in which CBCT and NE were not performed on the same day. The timing between the acquisition of CBCT DICOM and NE exam is critical since it is known that an increase in adenoid size can be correlated to an inflammatory and infectious episode(2), as well as with the level of immunological activity(111).

Density values, also known as gray thresholding, are still a challenge in the CBCT field, and to improve the airway research field, threshold values should be stated in every study. HU is not a standardized system, the HU value may not be the same if using the same CT machine but with a different technique, as well as if using a different machine.(58) Additional, it has been reported that the global thresholding pre-stablished in the automatic segmentation is the main cause of the largest variance compared to manual segmentation.(48, 112) The use of different thresholds even for different anatomical sites has been suggested.(48) Therefore, the need for adjustment of the threshold has been explored to obtain less variation on the results.(89)

We conducted a literature search on airway studies using Dolphin software and we found six studies(89, 108, 110, 112-114) that had reported adjustment of the threshold values. One study(89) obtained their scans through an I-CAT, and their scanning protocol was 120 kV, 5mA, 13x17cm field of view (FOV), 0.25mm voxel. In their study(89), they tested the sensitivity of 25, 50, and 70-75, and conclude that a threshold of 70 or over was the most accurate. In another study(113), the operator adjusted on a case-by-case basis, probably due to the anatomic abnormality of the craniosynostosis patient, since a previous study had stated that the gray values of air found in the nasal cavity differ from other areas due to the proximity of bones and mucous membranes.(48) In another study(108) two different thresholds (25 and 75) were used in two distinct samples where scans were obtained using different machines and scan protocols. Two studies(110, 112) did not report the value of the adjustment. Table 2.6 shows the summary of the literature reviews and more specific information about the studies.

In the present study, we adjusted the threshold to a value of 35 HU because a threshold of 50 HU overlapped the surrounding structures, and a threshold of 25 HU did not fully fill the lumen in some cases. A previous study(108) at our institution used a threshold of 25 HU in a different sample of patients but under the same scanning protocol. We assume these threshold's difference probably happened because those patients were wearing orthodontic apparatuses that can interfere with the CBCT phantom, consequently interfering at the gray thresholding.

Under similar conditions the selection of the cut off HU can have a major bearing in the volume measurement results as well as in the 3D surface. To simulate the impact of the changes we created a scenario with six threshold values (15, 25, 35, 50, 70 and 75 HU) in the same patient in the same landmark. These threshold values were based on previous airway studies(89, 108, 112, 114, 115) that reported the HU value. We observed results ranging from 4736 to 13163 in the surface volume, and in the sagittal area values ranging from 166 to 351, respectively from 15 to 75 HU. Additional, distortion of the 3D surface could be seen in threshold of 50 and over, as seen in Figure 2.10. Thus, caution should be taken since an inexperienced researcher would have unreliable results if any comparison in the measurements is made without standardizing the threshold sensitivity tool.

The 3D models were designed with a focus on the reproduction of actual nasopharyngeal anatomy, to demonstrate the lumen for airflow, but with some design adjustment, the same technique could be applied for different purposes. One example is the development of an algorithm, another would be that the use of the anatomical model for educational purpose for assessing the nasopharynx by adaptation of the technique and modification of the ROI making its use for basic scope navigation.

2.6. LIMITATIONS

The HU selection is still a limitation in the upper airway CBCT field. More studies exploring the effect of different–related techniques are needed.

2.7. CONCLUSION

The methodology for the generation of printed models of the nasopharynx's lumen and of the adenoid and anatomical surrounding areas based on CBCT's DICOM using Dolphin software is feasible and highly reliable.

2.8. FUTURE RESEARCH

- Further, we would like to assess the educational applicability of the 2D and 3D, one nasopharyngeal space reconstructed in multiple planes and the other a 3D printed model of the same area both to simulate the likely view that OHNS would have through NE.
- With our AD prototype as a reference standard we would be able to access the most reliable CBCT threshold for our institutional studies on airways, based on the volume of water necessary to fill the empty spaces of the prototype measured with a high-precision micropipette.
- A matched sample with similar age, height, weight, and BMI would compensate the confounders and improve the analyses and correlation of the volume parametric measurements with the grading size;
- Development of an algorithm for adenoid hypertrophy screening in CBCT.

2.9. Acknowledgements

We would like to thank to Dr. Miguel Lerner, a Brazilian OHNS specialist who gave us his expert opinion on how NE is performed, and valuable feedbacks on how we should improve our technique to better correlate with Nasal endoscopy technique. Also, Dr. Khal Ansari, a Canadian OHNS specialist for the feedback on the printed models.

We would like to thank the undergrad science student Lara Pereira for the second measurements for reliability. We would like to thank Dr. Hollis Lai for the statistical guidance

Support for the initiative was possible through the Centre of Teaching and Learning at the University of Alberta. Specially we thank the technician Rishi Jaipaul for the development support for the 3D printed models.

2.10. Figures & Tables

Figure 2. 1- Plane orientation and calibration

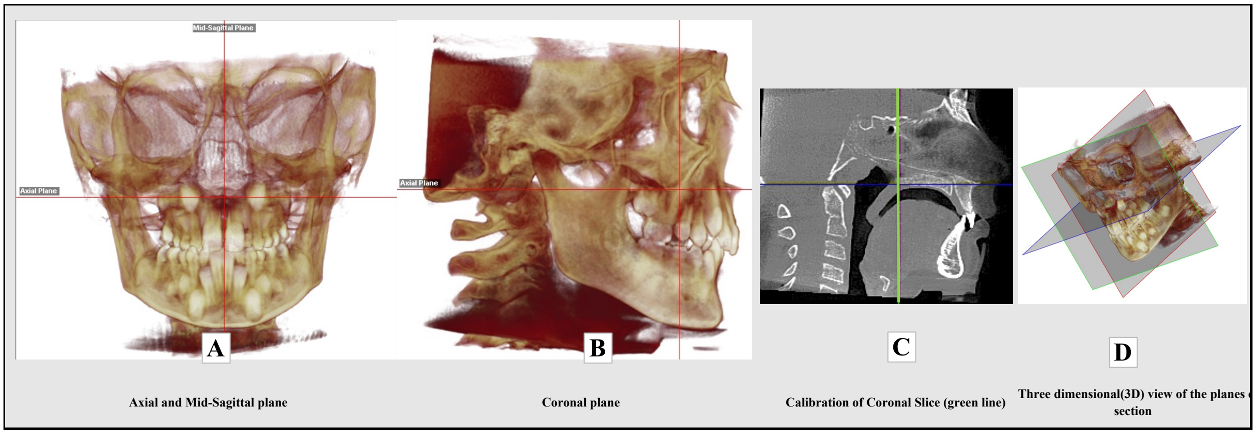

Figure 2. 2- Delimitation of the nasopharyngeal region of interest. Sagittal (A) and Axial (B) as well as the seed point and the airway lumen in yellow color.

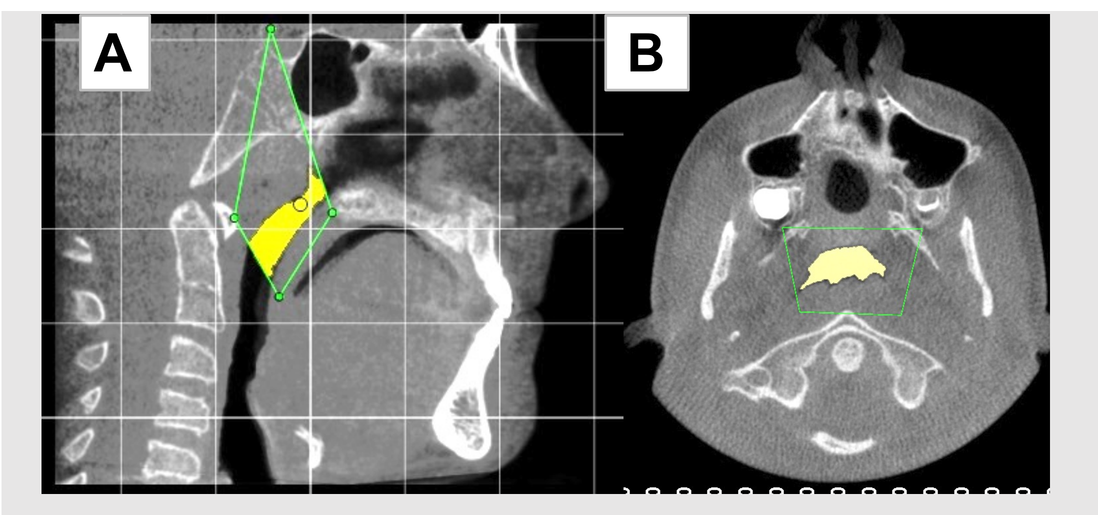

Figure 2. 3- Representation of the airway surface in the translucent hard tissue view. (A) sagittal view, (B) frontal view

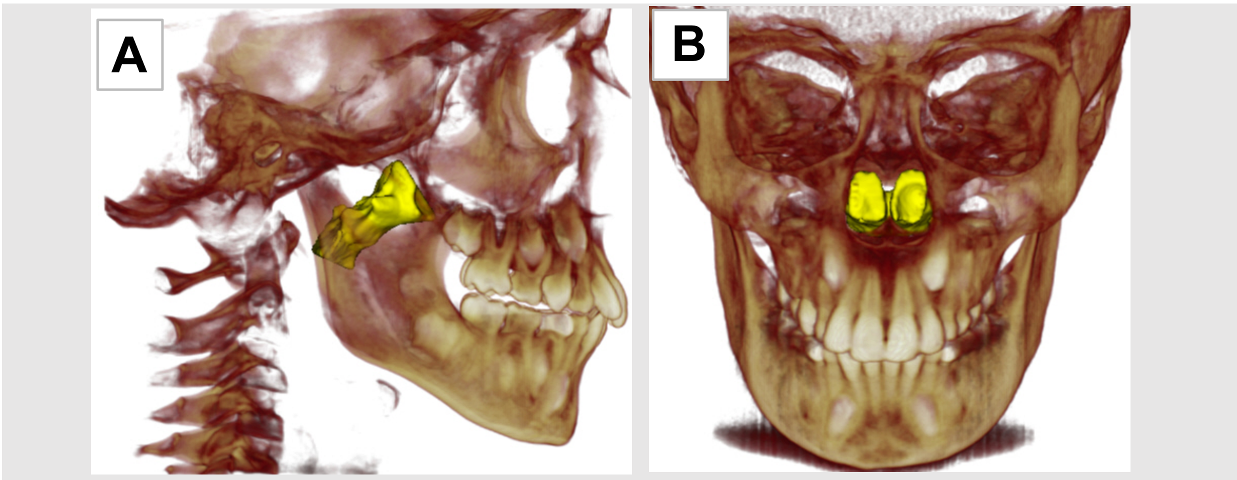

Figure 2. 4- Airway surface schematic representation

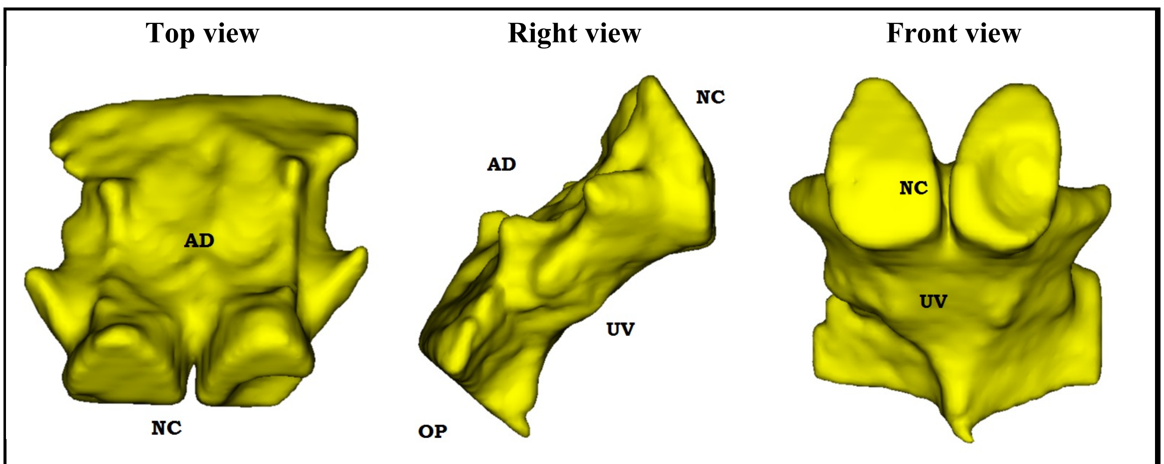

AD, adenoid; NC, nasal cavity; OP, oropharynx; UV, uvula

Figure 2. 5- Sagittal (A) and axial (B) landmarks for adenoid and surrounded area delimitation

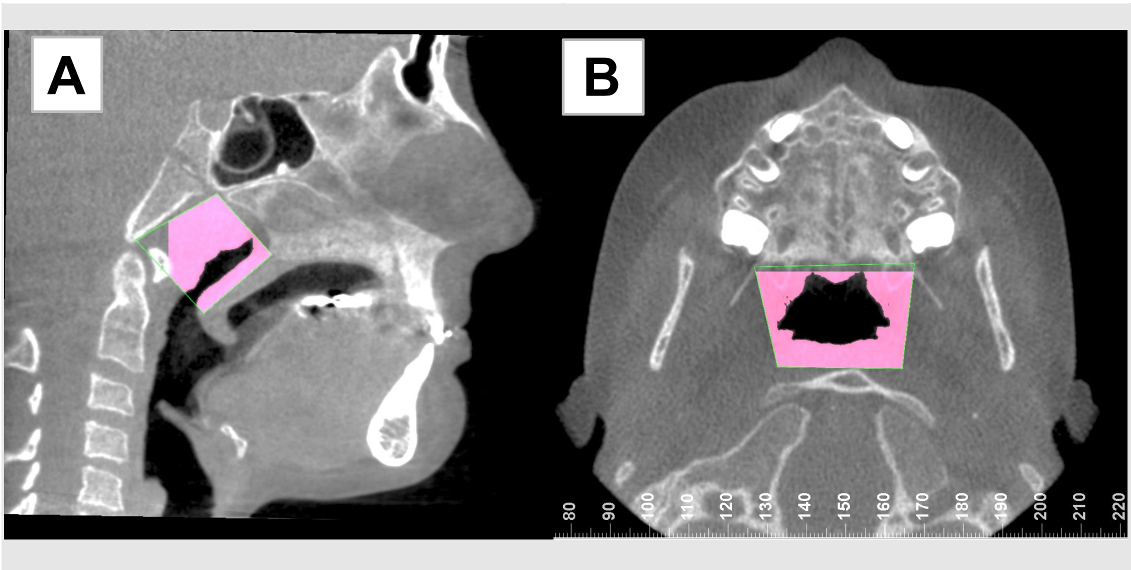

Figure 2. 6- Schematic representation of the adenoid mass surface

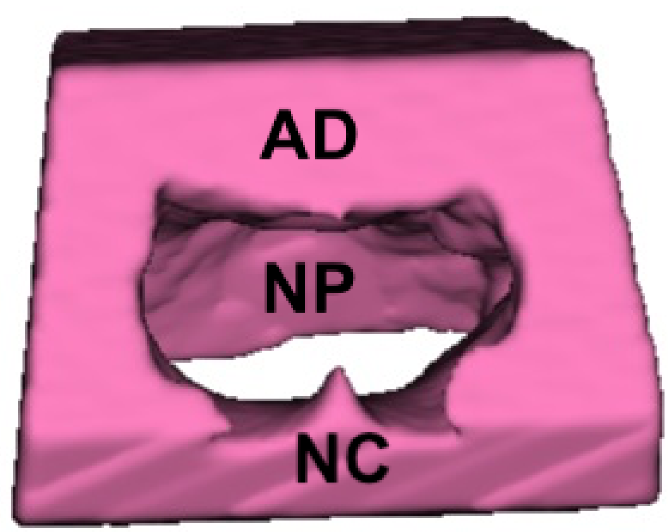

AD, adenoid; NP, nasopharynx; NC, nasal cavity.

Figure 2. 7- Superimposition of the two 3D models

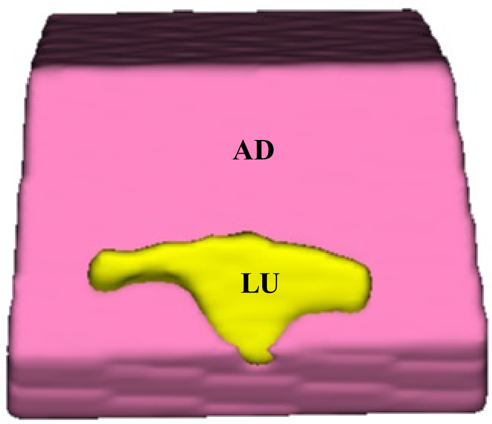

LU, Lumen of the airway; AD, adenoid and surrounded soft tissue

Figure 2. 8- Afinia H800 3D printer

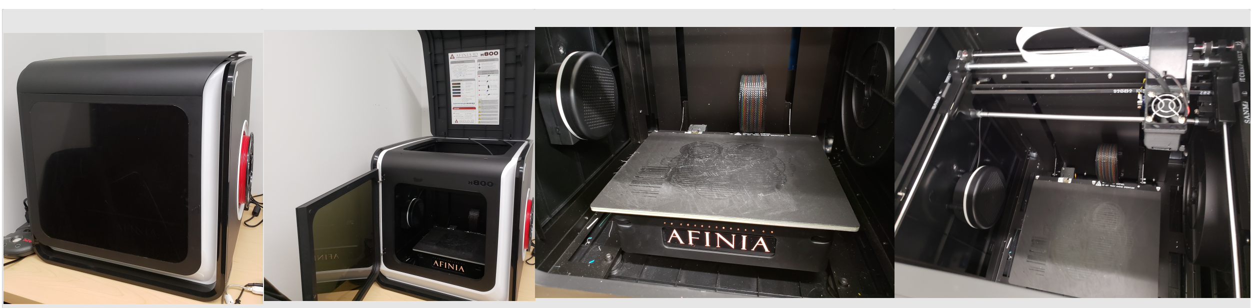

Figure 2. 9-3D printed models (prototypes)

Non enlarged

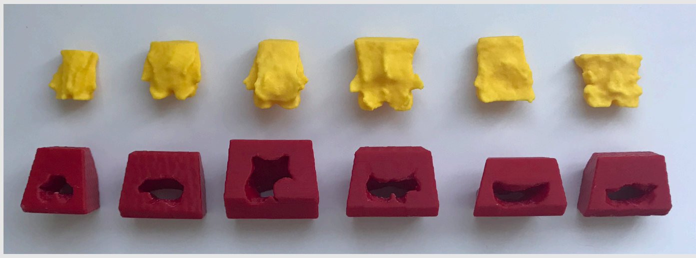

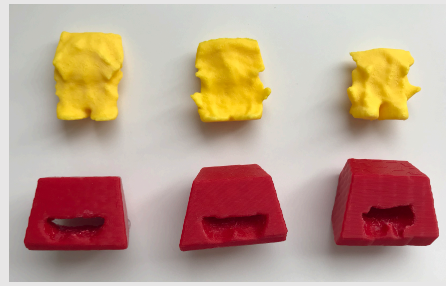

Grade 1 | Grade 2

Enlarged

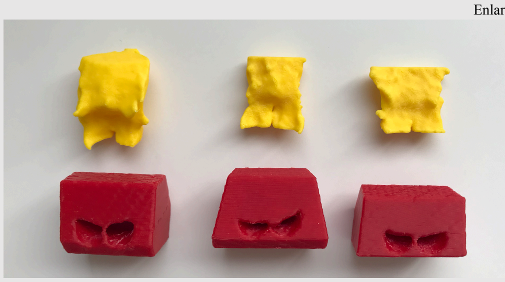

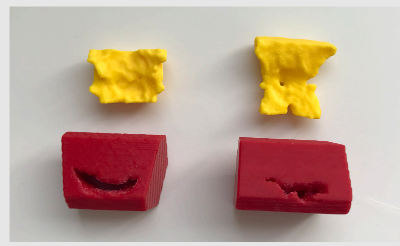

Grade 3 | Grade 4

Prototype yellow (LU-lumen); prototype Red (AD-adenoid & soft tissue). Grade 1: 25%; Grade 2: 25-50%; Grade 3: 50-75%; Grade 4: >75%

Figure 2. 10-Impact of sensitivity threshold adjustment in measurement and in 3D reconstruction surface in Dolphin software

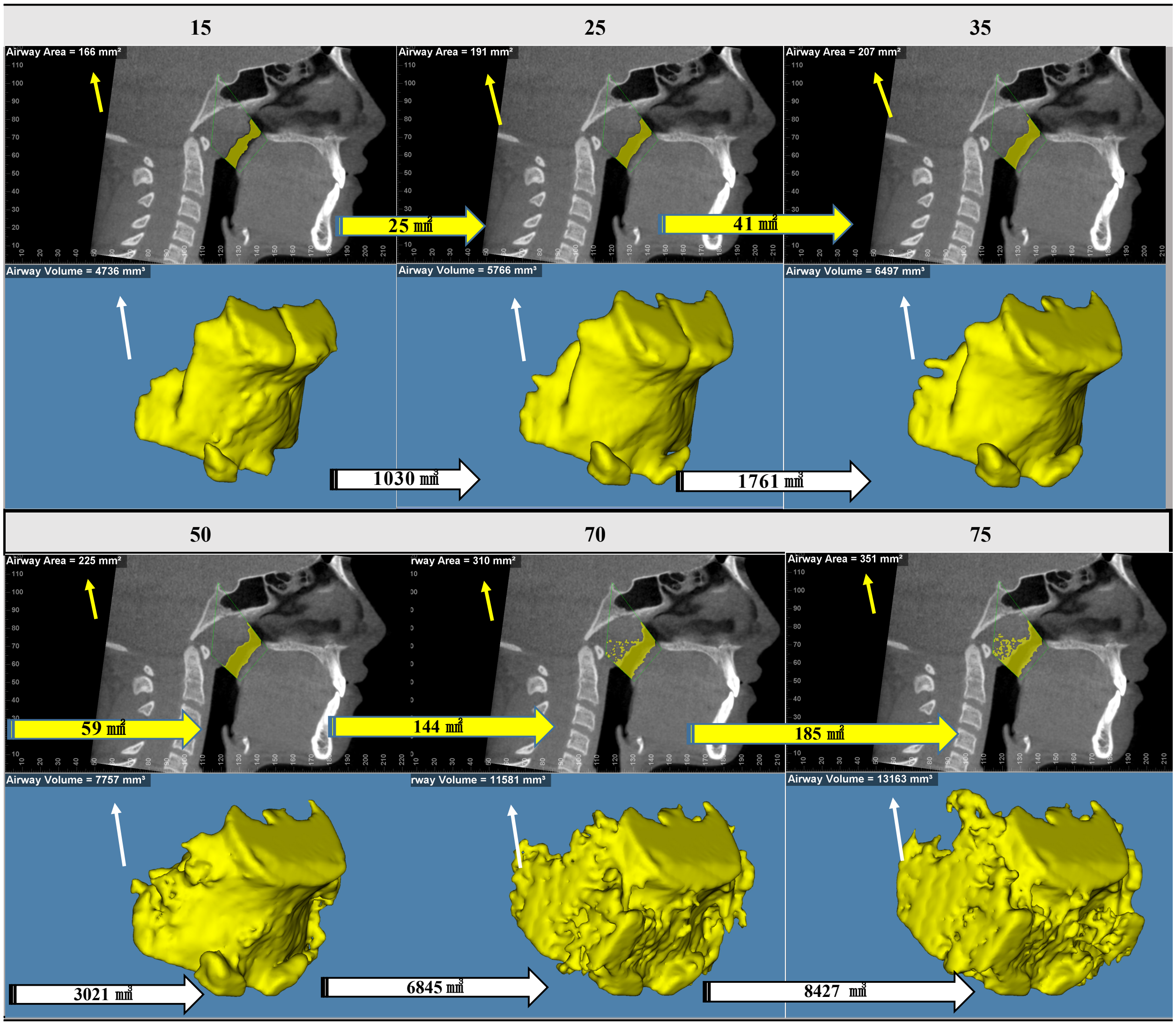

yellow arrow indicate the changing in area measurements, and white arrow indicate the changes in volume measurements.

Table 2. 1- 3D lumen surface (yellow color) in bottom, top, front and right view

	Bottom View	Top View	Front view	Right side view
Grade 1	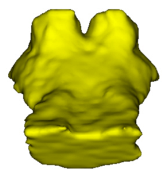	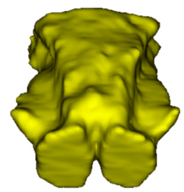		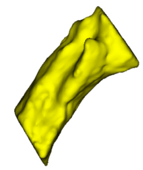
Grade 2	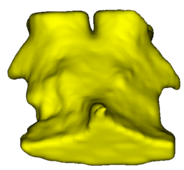	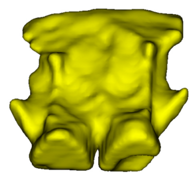	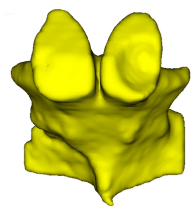	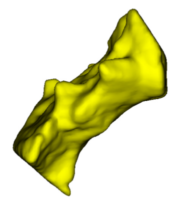
Grade 3	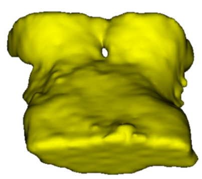	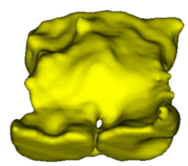	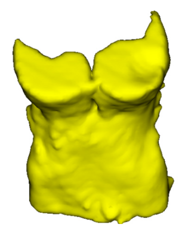	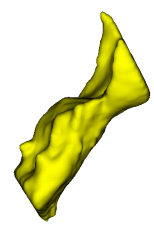
Grade 4	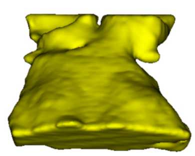	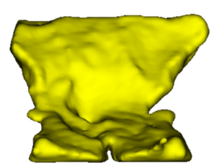	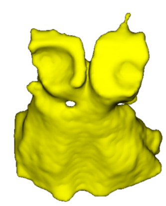	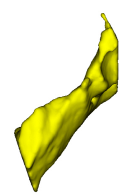

Grade 1: 25%; Grade 2; 25-50%; Grade 3: 50-75%; Grade 4: >75%

Table 2. 2- 3D Lumen surface plus hard tissue representation

Right view (RV)	Left view (LsV)	Front view (FV)	Top view	Bottom view
				
+ Hard Tissue				
				

Table 2. 3-Adenoid mass 3D surface and grade size classification

	Grade 1	Grade 2	Grade 3	Grade 4
Front view	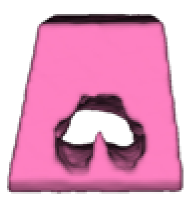			

Table 2. 4-3D Adenoid mass surface plus hard tissue representation

Right view (RV)	Left view (LsV)	Front view (FV)	Top view	Bottom view
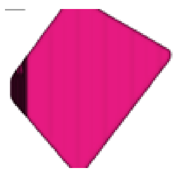	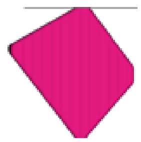	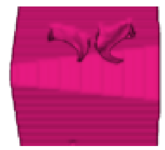	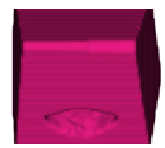	
+ Hard Tissue				
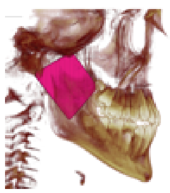			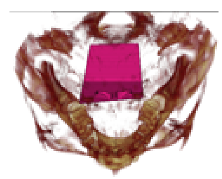	

Table 2. 5- Demographics and measurements (mean) of the selected sample

Type	n	Percent	Mean age (min, max, SD)	Sex Male (%) / Female (%)	LU volume	LU axial area	AD volume	AD axial area
Grade 1	6	42.90%	10.995 (7.2-15.7; SD 3.73)	6 M (100%)	6757.67	327.5	21195.67	638
Grade 2	3	21.40%	8.676 (7.2-10.1, SD 1.46)	3 (100%) / 0 (0%)	4487.33	211.67	13339.67	652.33
Grade 3	3	21.40%	9.533 (8.4-11.1, SD 1.39)	2M (67%) / 1F (33%)	4439	219.67	17879.67	595
Grade 4	2	14.30%	14 (14-14,0.0)	1 M (50%) / 1F (50%)	5158	188	25302.5	665.5
Non-enlarged	9	64.30%	10.22 (7.7-15.7, SD 3.25)	9 M (100%)	6000.89	288.89	18577	642.78
Enlarged	5	35.70%	11.32 (8.4 - 14, SD 2.63)	3M (60%) / 2F(40%)	4726.6	207	20848.8	623.2
Overall sample	14	100%	10.614 (7.2-15.7,SD 2.99)	12M (86%) / 2F(14%)	5545.79	259.64	19388.36	635.79

n, number; min, minimum; max, maximum; SD, standard deviation; %, percentage; Lu, lumen of the nasopharyngeal airway; AD, adenoid and soft tissue region

Table 2. 6- Summary of the literature review in Dolphin software and interactive Imaging thresholding tool

IIT	Title	Author	Year	Country	Field	Software	Ct machine	Voxel	Kv	mA	FOV	Time	Threshold sensitivy
Adjusted	Is the airway volume being coorrectly analyzed?	Alves, M et al.	2012	Brazil	Orthodontics	Dolphin	I-Cat	0.25	120	5 mA	13x17cm	40 second	25,50,70-75
	Imaging software accuracy for 3-dimensional analysis of the upper airway	Weissheimer et al.	2012	Brazil/USA	Orthodontics	Dolphin	I-cat	0.3	120	8 mA		40 second	NR
	Three-dimensional cone beam computed tomography definition of the anatomical subregions of the upper airway: a validation study	Guijaro-Martinez & Swennen	2013	Spain	Oral & maxillofacial surgery	Dolphin	I-cat	0.4	120	48 mA	17 X 22 cm	2 x 20 sec	70 (48-81)
	Measuring Upper Airway Volume: Accuracy and Reliability of Dolphin 3D Software Compared to Manual Segmentation in Craniosynostosis Patients	De Water et al.	2014	Netherlands	Oral & maxillofacial surgery	Dolphin	NR	1.25	NR	NR	NR	NR	NR
	Volumetric reconstruction and determination of minimum crosssectional area of the pharynx in patients with cleft lip and palate: comparison between two different softwares	Pinheiros et al.	2018	Brazil	Oral & maxillofacial surgery	Dolphin	NR	NR	NR	NR	13 cm	NR	Individuaized for each patient
	Effects of bimaxillary orthognathic surgery on pharyngeal airway and respiratory function at sleep in patients with class III skeletal relationship	Tepecik, Ertas & Akgun	2018	Tyrkey	Oral & maxillofacial surgery	Dolphin	NewTom	0.5	110	15 mA	13 x 17	5.4 sec	50
	lopment of a 3D printed model of the nasopharyngeal adenoidal area using CBCT	Thereza-Bussolaro et al.	2019	Canada	Oral & maxillofacial surgery	Dolphin	I-cat	0.3	110	6.19 mA	12 in	3.9 second scan	35
	Does pterygomaxillary disjunction in surgically assisted rapid maxillary expansion influence upper airway volume? A prospective study using Dolphin Imaging 3D	Medeiros et al.	2017	Brazil	Oral & maxillofacial surgery	Dolphin	I-cat	0.4	120	3-8 mA	22 x 16	NR	25
	Pharyngeal Dimensional changes in Class II malocclusion treatment when using Forsus® or intermaxillary elastics - An Exploratory Study	Thereza-Bussolaro et al.	2019	Canada	Orthodontics	Dolphin	I-cat	0.3	110	6.19 mA	12 in	3.9 second scan	25
	Pharyngeal Dimensional changes in Class II malocclusion treatment when using Forsus® or intermaxillary elastics - An Exploratory Study	Thereza-Bussolaro et al.	2019	Canada	Orthodontics	Dolphin	I-cat	0.4	110	6.19 mA	16 x13 cm	3.9 second scan	75
Not Adjusted	The influence of craniofacial morphology on the upper airway dimensions	Indriksome	2015	Latvia	Orthodontics	Dolphin	I-cat	0.4	120	5 mA	13 x 17	20 seconds	NO
	Reliability of a method to conduct upper airway analysis in cone-beam computed tomography	Souza et al.	2013	Brazil	Orthodontics	Dolphin	I-cat	0.4	120	36.9 mA	13 x 23 cm	40 seconds	
	Correlation and reliability of cone-beam computed tomography nasopharyngeal volumetric and area measurements as determined by commercial software against nasopharyngoscopy-supported diagnosis of adenoid hypertrophy	Pacheco-Pereira et al.	2017	Canada	Orthodontics	Dolphin	I-cat	0.3	110	6.19 mA	12 in	3.9 second scan	
	Accuracy and reliability of cone-beam computed tomography for airway volume analysis	Ghoneima and Kula	2013	Egypt	Orthodontics	Dolphin	I-cat	0.4	NR	NR	13 cm	3.9 second scan	

IIT, Interactive Imaging Threshold tool; Kv, tube voltage; mA, tube current

Chapter 3: Validation of the use of a 3D printed model depicting Adenoid Hypertrophy in comparisons to a Nasoendoscopy- based grading assessment

INTRODUCTION

Signs of SDB are considered relatively common among children. SDB represents a myriad of related disorders ranging from snoring to upper airway resistance syndrome (URS) to an obstructive sleep apnea syndrome (OSAS).(2) Poor school performance, gasping for breath at night, and snoring are some of the signs reported by caregivers. A narrow upper airway (UAW) has been associated to pediatric OSA, and one of the more likely cause is adenotonsillar hypertrophy. Adenoidectomy is sometimes indicated when it is associated with nasopharyngeal obstruction.(116) Thus, identification of an enlarged adenoid in childhood would streamline the referral of appropriately selected cases to an OHNS, leading to early treatment of affected children when indicated.

The usefulness of diagnostic tools and referral algorithms for the detection of enlarged adenoid and nasopharyngeal obstruction has been developed and investigated over the years.(102) The evaluation of nasopharyngeal obstruction is done either estimated subjectively by direct visualization or objectively by mean of direct measurement in pertinent imaging.(102) The antrum-adenoidal space, the ratio between adenoid, the nasopharyngeal space, and the measured choanal obstruction space (MCO) are examples of objective measurements. Adenoid grading methods also varies from simply categorical "normal or enlarged"(117, 118), "small, moderate and large"(119) to ordinal scales in three(120) or four grades.(42)

Flexible fiberoptic nasal endoscopy (NE) is an imaging method used for multiple purposes in a routine OHNS practice.(8) It has shown a sensitivity of 92% and specificity of 71%

for adenoidal hypertrophy obstruction detection.(121) Cone beam computed tomography (CBCT) is becoming part of the routine of orthodontic records and it has been explored for evaluating adenoid size(13, 15-17) in comparison to NE. Therefore, digital images (DICOM) would be readily available for adenoid hypertrophy assessment in some cases when there is suspicion of UAW obstruction. The exploration of 3D print outs of the nasopharyngeal area has not been explored, it could streamline the diagnostic process, especially in cases where the patients have already a recent CBCT in which a hypertrophic adenoid is suggested. It would also substitute the need for an additional NE in selected cases and would be useful in remote regions where the access to an OHNS specialist is absent.

The final stage of this research project is to validate the use of a 3D printed model depicting adenoid hypertrophy based on the pediatric OHNS participants assessment. Our hypothesis is that the grades obtained from the OHNS participants will be similar to those on the record as previously determined by an OHNS assessing the area through NE.

3.1. MATERIAL AND METHODS

3.1.1. Study design and protocol

Four depictions (two 2D, and two 3D) of the nasopharyngeal adenoidal area were created per included participant from the sample of available cases (Figure 3.1). The manufacturing techniques of the prototypes were described in Chapter 2. A flowchart of the sampling reasoning and study design can be seen in **Appendix A.**

A prospective protocol for validation of the 3D printouts was proposed and ethical approval was obtained through the research ethics committee at the university of Alberta under protocol number Pro00082445 (**Appendix B**).

3.1.2. DICOM Sampling

The selected sample consisted of CBCT scans of 14 children representing grades 1, 2, 3, and 4 nasopharyngeal obstruction, according to a previously NE-graded classification by a licensed OHNS.(15) A total of 12 boys and 2 girls with a mean age of 10.61 years (7.2-15.7 years old, SD,2.99) were considered. The selected sample consisted of 6 cases of grade 1 (42.9%), 3 cases of grade 2 (21.4%), 3 cases of grade 3 (21.4%), and 2 cases of grade 4 (14.3%), based on the distribution of the Parikh grading system classification.(42) The prevalence of AH in this study was 36%, which is very similar to the percentage prevalent in the pediatric population, 34.46%.(41) Converting the sample to non-enlarged and enlarged, the sample ended up to having 9 cases in the non-enlarged group with a mean age of 10.22 years (SD 3.25) and 5 cases in the enlarged group with a mean age of 11.31 (SD 2.63). Table 2.1 in chapter 2 of this thesis research project shows the demographics and descriptive statistics of the selected sample. **Appendix A** contains a flowchart of sample selection, inclusion, exclusion criteria, and eligibility.

3.1.3. OHNS Sampling

A sample of two evaluators was recruited at the Department of Otolaryngology-Head and Neck Surgery of the Faculty of Medicine and Dentistry of University of Alberta, In Canada. The participants had to be registered OHNS specialists in the province of Alberta. All were sent a letter of invitation by email **(Appendix C).** The participants were invited to participate, and to avoid any undue pressure, it was made clear through informed consent that the study was voluntary (**Appendix D**). The participants were free to withdraw from the study at any time up until the end of the data collection. All the material from the data collection was anonymized.

3.1.4. Reference Standard

Our reference standard method was based on previously performed NE exams and details are described in a previous study.(15)

3.1.5. Procedure

The 3D depictions of the pharyngeal adenoidal obstruction included two different anatomic regions of the nasopharyngeal airway, lumen (LU) and adenoid mass (AD). LU and AD were visualized in 2D - pictures- and in 3D – prototypes. One member of the research team (CTB) took the 3D depictions alongside with a guidance sheet (**Appendix E**) and with a cheat sheet containing the grading system (**Appendix F**) - to one participant at a time. Each participant was assessed two times with an interval of one week between the assessments.

The 3D prototypes were coded in a way that the same prototype received two different codes depending on the day it was assessed, allowing us to analyze the intra-rater reliability. Chapter 2-figure 2.9- of this thesis research project shows a picture of the prototypes.

The two-day assessments involved grading the level of obstruction of the nasopharynx, following a previous validated classification of four grades of AH through NP assessment using the Parikh et al., 2006 grading system.(42) The participants were given different sheets and codes, according to the day of assessment, as follows:

- Assessment day 1:
  - ⇒ Grading through the airway surface model printed on a paper sheet labeled “A” (Codes: A through N) (Figure 3.2);
  - ⇒ Grading through the adenoid mass surface model printed (Codes: O through CC), on a paper sheet labeled “A1" (Figure 3.3)
  - ⇒ Grading the actual airway prototype (Codes: PLU1 through PLU14); and grading the adenoid mass prototypes (Codes: PAD1 through PAD14), using a paper sheet labeled “P1” (Table 3.2).
- Assessment day 2:
  - ⇒ Grading through the airway surface model printed (Codes: DD through QQ) on a paper sheet labeled “B” (Figure 3.4);
  - ⇒ Grading through the adenoid mass surface model printed (Codes: RR through AN), on a paper sheet labeled “B1” (Figure 3.5);
  - ⇒ Grading the actual prototypes: airway (Codes: LL, L, U, S); and grading the adenoid mass prototypes (Codes: PP, A, TH, Z), using a paper sheet labeled "P2” (Table 3.2).

3.1.6. Statistical analysis

Statistical analyses were done using the Statistical Package for the Social Science (IBM, version 25; SPSS Inc., Armonk, NY, USA). Microsoft® Excel for Mac, version 15.27 was used to obtain any necessary averages and graphs.

The intraclass correlation was used to assess the intra- and inter-reliability between the two evaluators. The analyses were performed on the 4-point grading system according to the

Parikh(42) grading system, additionally, the data were converted and coded based on the clinical classification of non-enlarged (grade 1 and grade 2) - code 0 - and enlarged (grade 3 and 4) - code 1. We followed the interpretation of poor agreement = 0-0.2; fair agreement = 0.3-0.4; moderate agreement = 0.5-0.6; strong agreement = 0.7-0.8; almost perfect agreement = >0.8.(122)

The validity of our depictions were analyzed through comparison (accuracy and correlation) between our tools results and the reference standard (NE). To calculate the sensitivity, specificity, positive predictive value (PPV), and negative predictive value (NPV), we clustered the results in non-enlarged and enlarged. Cross-tab and Pearson's c-test were performed.

MANOVA were performed to find power description and effect size (partial eta-squared - $\boldsymbol{\eta_p^2}$) of the study. The level of significance and confidence interval (CI) was set at 0.05.

3.2. RESULTS

One hundred and twelve (n=112) adenoidal nasopharyngeal assessments were done by each OHNS participating in this study. A total of 28 OHNS were invited, 2 agreed to participate. The participants evaluated the adenoid size of 14 patients represented in 4 different ways: LU 2D, AD 2D, LU 3D, AD 3D as shown in figure 3.1 respectively A, B, C, D. Overall, an almost perfect overall agreement was observed for the 112 possible agreements in adenoid grading from the two examiners scoring in grading system, inter- rater reliability ICC mean= 0.88 (95% CI, 0.76 - 0.95), and in the clinical classification of enlarged and non-enlarged, ICC mean = 0.87 (95% CI, 0.75 – 0.95). The lower bound of agreement still implied the "strong agreement" grading.

3.2.1. Statistical Power

Statistical power analysis of the evaluations based on the grading system(42), was high for each shared visualization tool. Based only on enlarged and non-enlarged classification, it was also high for all 3D depictions (> 0.92), but 0.84 for LU 3D which is still a high power. Effect size was large for all 3D depictions in the grading classification, although for the clinical classification effect size was large for AD 3D, medium for AD 2D, but small for LU 2D and LU 3D, and as seen in Table 3.3.

3.2.2. Reliability

The degree of consistency with OHNS evaluated the depictions were observed through intra-rater reliability by grading score and by clinical classification as below:

By grading system

Intra-reliability (OHNS 1):

- LU 2D picture ICC = 0.00; CI: 0 – 0.55; NS (poor)
- AD 2D picture ICC = 0.97; CI: 0.92 – 0.99; P<0.001 (almost perfect)
- LU 3D prototype ICC = 0.86; CI:0.57–0.95; P<0.001(almost perfect)
- AD 3D prototype ICC=0.84; CI:0.52 – 0.95; P<0.001 (almost perfect)

Intra-reliability (OHNS 2):

- LU 2D picture ICC = 0.88; CI: 0.63 – 0.96; P<0.001 (excellent)
- AD 2D picture ICC = 0.93; CI: 0.79 – 0.98; P<0.001 (excellent)
- LU 3D prototype ICC = 0.64; CI: 0.0 – 0.88; P<0.001 (moderate)
- AD 3D prototype ICC = 0.71; CI: 0.12 – 0.91; P<0.001 (strong)

By clinical classification

Intra-reliability (OHNS 1):

- LU 2D picture ICC = 0.92; CI: 0.78 – 0.98; $P<0.001$ (excellent)
- AD 2D picture ICC = 0.93; CI: 0.78 – 0.98; $P<0.001$ (excellent)
- LU 3D prototype ICC = 0.93; CI: 0.78 – 0.98; $P<0.001$ (excellent)
- AD 3D prototype ICC = 0.75; CI: 0.23 – 0.91; $P<0.001$ (good)

Intra-reliability (OHNS 2):

- LU 2D picture ICC = 0.93; CI: 0.78 – 0.98; $P<0.001$ (excellent)
- AD 2D picture ICC = 0.93; CI: 0.78 – 0.98; $P<0.001$ (excellent)
- LU 3D prototype ICC = 0.73; CI: 0.19 – 0.913; $P<0.001$ (good)
- AD 3D prototype ICC = 0.16; CI: 0.0 – 0.73; NS (poor)

We also verified the agreement between evaluators thought inter-reliability. In summary, inter-rater reliability by the grading system according to Parikh(42), a moderate but not statistically significant agreement was found for LU 2D, a statistically significant and almost perfect agreement was observed for AD 2D, a moderate and also significant agreement for LU 3D was found, and a statistically significant and strong agreement was observed for AD 3D.

For the clinical classification of enlarged and non-enlarged AH, poor agreement was observed for LU 2D, a statistically significant and almost perfect agreement for AD 2D, a not statistically significant and poor agreement for LU 3D and a statistically significant and good agreement for AD 3D, as seen in Table 3.4.

3.2.3. Accuracy

3D Depictions by grading system versus(vs) Reference Standard

- LU 2D vs NE: ICC=0.54, CI: 0 – 0.85; NS (moderate)
- AD 2D vs NE: ICC=0.75, CI: 0.27 – 0.92; P<0.001 (strong)
- LU 3D vs NE: ICC=0.57, CI: 0 – 0.86; NS (moderate)
- AD 3D vs NE: ICC=0.88, CI: 0.63 – 0.96; P<0.001(almost perfect)

3D Depiction by Clinical Classification vs Reference Standard;

- LU 2D vs NE: ICC=0.0, CI: 0 – 0.58; NS (poor)
- AD 2D vs NE: ICC=0.62, CI: 0 – 0.88; P<0.005 (moderate)
- LU 3D vs NE : ICC=0.57, CI: 0 – 0.86; NS (moderate)
- AD 3D vs NE : ICC=0.83, CI: 0.44 – 0.94; P<0.001 (almost perfect)

In summary, by the grading system according to Parikh(42), moderate but not statistically significant accuracy was found for LU 2D, a statistically significant and strong accuracy was observed for AD 2D, a moderate but not significant accuracy was observed for LU 3D, and a statistically significant and almost perfect accuracy was found for AD 3D.

Accuracy by the clinical classification of enlarged and non-enlarged, was poor and not statically significant for LU 2D, statistically significant and moderate for AD 2D, also moderate but not statically significant for LU 3D, and statistically significant and almost perfect for AD 3D.

Therefore, both 2D depictions (LU 2D and AD 2D) showed a decrease in accuracy under clinical classification vs grading system.

3.2.4. Correlation

3D Depictions vs NE Correlation analysis

- LU 2D vs NE: r = - 0.25, NS (no correlation)
- AD 2D vs NE: r = 0.45, NS (moderately strong correlation)
- LU 3D vs NE: r = 0.38, NS (weak correlation)
- AD 3D vs NE: r = 0.69, P < 0.01 (strong correlation)

3.2.5. Sensitivity and Specificity

- LU 2D sensitivity 25 %, CI: 0-40%; Specificity 78%, CI: 33.30 – 155%
- AD 2D sensitivity 80%, CI: 80-80%; Specificity 61%, CI: 55.60 – 66.70%
- LU 3D sensitivity 55%, CI: 40-60%; Specificity 64%, CI: 55.60 – 77.80%
- AD 3D sensitivity 95%, CI: 80-100%; Specificity 58%, CI: 22.20 – 88.90%

Sensitivity and Specificity (without outliers)

Only two 3D depictions showed outliers:

- LU 2D sensitivity 33%, CI: 20-40%; Specificity 52%, CI: 33.3 – 77.80%
- AD 3D sensitivity 100%, CI: 100%; Specificity 70%, CI: 55.6 – 88.90%

In summary, a low sensitivity and high specificity was found for LU 2D, a high sensitivity and high specificity was found for both AD 2D and AD 3D, and a low sensitivity and low specificity for LU 3D. LU 2D showed more non-enlarged cases than the actual number of negative cases, that is why a 155% of upper bounder in the CI, having an average of 75% of false negative cases.

3.2.6. Positive and negative predictive value

- LU 2D PPV= 22%; NPV= 59%, without outlier: PPV= 29%
- AD 2D PPV= 54%; NPV= 85%
- LU 3D PPV= 47%; NPV= 72%
- AD 3D PPV= 60%; NPV= 97%; without outlier: PPV= 66%

In summary, in a sample with an AH prevalence of 36%, with a positive test for enlarged adenoid the chances of a patient who actually have an enlarged adenoid to be tested positive increases from 36% to 54% in the AD 2D, to 47% in the LU 2D, and to 66% in the AD 3D. Nevertheless, the chances of a patient who actually has an enlarged adenoid to test positive for LU 2D decreases from 36% to 29%.

Regarding NPV results, the chances of the patient with a negative test for enlarged adenoid who actually does not have enlarged adenoid increases from 64% to 85% for AD 2D, to 72% for LU 3D, and to 97% for AD 3D. Nevertheless, the chances of a healthy patient to be tested as "healthy" decreases from 64% to 59% in LU 2D.

3.3. DISCUSSION

The need for early referral, diagnostic and management of AH in children has been suggested in the literature over the years. Dentists should consider the possibility of referring the patient for a full OHNS assessment if any potential nasopharyngeal obstruction is identified. The clinical assessment of the upper airway space is usually comprised of direct clinical visualization and symptoms such as snoring, mouth-breathing and obstructive breathing during sleep should also be considered for referral.(1)

Direct clinical visualization of some pharyngeal areas can be limited, alternative nasopharyngeal image approaches could be used to improve the screening for potential obstruction. The exploration of 3D technology of computational tomography and the development of valid 3D printed models may improve the assessment of adenoid obstruction and may have a significant teaching potential as an adjunct to CT imaging training and referral training to OHNS specialists.

Regarding overall inter-examiner assessment of adenoid size, our study reached an almost perfect agreement. Therefore, it was superior to previous studies using CBCT(16, 17), respectively ICC =0.69 and ICC of 0.39 for inter-examiner assessment. In addition, our results were similar to the agreement observed in the study by Major(15) which presented an ICC of 0.80.

Validity is the degree to which a test measures what it is intended to measure, the determination of validity for any test instrument can be made in a variety of contexts. In our study we validate our depictions by criterion-relate validity, verifying the correlation and accuracy of our tools results against a NE based grading assessment by and OHNS as reference standard. Additionally, as required by specifically designed screening tools, we verify the validity of our tools by evaluating its ability to accurately assess the presence and absence of AH. Therefore, the validity of our 3D depictions was based on accuracy, sensitivity, and specificity.

The current reference standard validation study for NE, the Parikh(42) grading system, is a subjective method in which an inter examiner agreement of 0.71(kappa) among physician and residents was observed. The authors did not evaluate intra-rater reliability (consistency), their validation was based on interrater agreement, but no comparison with a reference standard was performed. Therefore, no sensitivity, specificity, PPV or NPV were provided. This is unusual, since in previous grading validation studies(117-120, 123) reference standards were continuously used to provide correlation analyses. This information limitation on the Parikh study restricts the comparison of our 3D depiction tools with our reference standard test.

Regarding individual visualization tool's performance – LU 2D, AD 2D, LU 3D, and AD 3D - both the picture (AD 2D) and the prototype (AD 3D) representing the adenoid and soft tissue were in general terms reliable (ICC > 0.75) and accurate (comparing with our reference standard, ICC >0.80). This is probably because the examiner can subjectively calculate the lumen space comparing it to adjacent anatomic structures. Besides, the "AD assessment'' type of view is similar to the view OHNS has on the NE exam; thus, the examiners were more familiar with this view.

Various methods have been developed over the years to assess adenoid sizes(8, 70), mostly based on the available space (lumen) in the nasopharynx around the adenoids, and not specific on the real size of the adenoid tissue. The assessment of adenoid through NE and classification are usually determined subjectively and estimating the extent of encroachment by the adenoid on the nasopharyngeal airway. Our methodology evaluated the performance of two different depictions, lumen and adenoid tissue. And the second, showed the better performance, probably because it allowed a view of the relationship between the adenoid and the nasopharynx space available.

It is interesting to observe that although OHNS constantly agreed in some cases, their classification differed from the available reference standard in multiple scenarios. Overall 7 cases of this specific disagreement could be observed as follow: 2 cases (L and N, figure 3.2) in the LU 2D; 2 cases (V and W, figure 3.3) in the AD 2D; 2 cases in the LU 3D case (PLU5 and

PLU10), and only one case (PAD 8) of disagreement in the AD 3D. Understandably, when we look at the prototypes PLU5, PLU10, PAD 8 (figure 3.6) the participant's opinion agreed with the OHNS. Thus, those cases would be reconsidered after an OHNS specialist clinical consultation if referred.

In comparison with the reference standard NE assessment, AD 3D and AD 2D showed the better statistical results in both grading systems and clinical classifications, furthermore AD 3D presented almost perfect agreement in both of them. Additionally, AD 2D and AD 3D visualization tools showed respectively a moderately and strong correlation with our reference standard. Therefore, both AD 2D and AD 3D visualization tools allowed for an accurate grading of the adenoidal nasopharyngeal area. We assume that is probably due to the similarity of this view with the NE view, in which they are habituated to. These results can be better visualized in Table 3.5.

Between the two depictions of the adenoid tissue and soft tissue - AD picture and prototype - the later presented slightly better results for accuracy, correlation, specificity and sensitivity, as seen in Table 3.5. We hypothesize that this could possibly be due to the 3D characteristic of the prototypes which allowed touching and looking at the real depth of the nasopharyngeal and the adenoid along with its relationship with adjacent structures. Although, while the prototype showed better performance, in a clinical setting the access to 3D printers is limited, therefore the application of AD 2D by health professionals would be more realistic and would *per se* help streamline the affected patients to the care of a specialist.

The diagnostic capability of the assessed visualization tools as a diagnostic test for AH was statistically calculated. Sensitivity is the ability of a test to identify the adenoid enlarged cases, while specificity is the test's ability to identify all non-enlarged cases. Excellent sensitivity and specificity was observed for the AD 3D (100%, 70%). A sensitivity of 100% means that our tool was able to identify all the cases with AH, and that the number of false negatives were low. Major et al., 2014(70) stated that lower sensitivity is acceptable for AH, at the same time the authors contradict themselves stating that "low rate of false-negative cases" is preferred to not miss the undiagnosed patients. We believe the authors meant a higher sensitivity, is preferred not a low sensitivity, because it leads to a low rate of false negative cases. After all, a link between HA and upper airway obstruction has been reported.(9, 33), such obstruction may lead to SBD, to a compromised quality of life and general physical conditions.(8, 34), and that a delay in treatment also increases the need for more complex medical interventions.(19, 20) Therefore, the AD 3D depiction seems to have achieved the study goal for correctly identifying enlarged adenoids, and also beat a previously(70) set up cutoff values for specificity at 90%.

The accuracy of adenoid tests has been investigated in a systematic review.(70) The author found a great variability between diagnostic tools compared to NE, for specificity ranging from 34 to 97%, and for sensitivity, from 22 to 100%. The best results were seen in a video fluoroscopy study(109) -100% sensitivity and 93% specificity, and MDCT study- 92% for sensitivity and 97% for specificity. But they carry the disadvantage of a higher radiation compared to CBCT. On the other hand clinical examination does not expose the patient to ionizing radiation, but showed a poor sensitivity of 22%, and an excellent specificity of 88%.(70) Thus, since a CBCT is not an independent exam, meaning, it would always be complemented by a specialist consultation and clinical examination, it would definitely improve the low sensitivity of the clinical examination.

The performance indices of PPV and NPV were also analyzed. To easily verify the usefulness of our 3D depictions in a clinical setting, we approximately mimic our sample with the prevalence of AH in the pediatric population (34.46%).(41) To do so, we randomly selected 9 non-enlarged cases and 5 enlarged adenoid cases, thus the prevalence of AH in our group was 35.7%. Hence, our final sample consisted of 14 patient-cases which gave us a sample size of 56 different printed cases, as follow: 14 LU 2D (surface picture), and 14 AD 2D (surface picture), 14 LU 3D (prototype), 14 AD 3D (prototype).

In a population-based setting, the probability of patients who truly have enlarged adenoid (PPV) to be identified by the 3D depictions were higher for the AD 3D with a PPV between 60-66%; AD 2D showed a good probability (PPV= 54%) as well. The probability of patients who truly do not have enlarged adenoid (NPV) to be identified by our tools was 97% for AD 3D, and 85% for AD 2D, and 72% for LU 3D. The worst performance was observed for the picture of the lumen (LU 2D) PPV= 22-29% and NPV = 59%, since their probability was below the prevalence of enlarged (36%) and non-enlarged (64%) in the population. Table 3.5 shows the values for all 3D depictions.

Previous studies(101, 109, 124-126) assessed the correlation of their index (radiographic) test when comparing to an NE as a reference standard. They were systematically reviewed(102), and the best correlation (r = -0.793) was found in a teleradiography study.(127) Nevertheless, this study(127) was not peer review indexed, besides, their sensitivity value was not remarkable, 75%. A previous study(13) of the volume and cross-sectional 3D and 2D measurements with a NE reference standard showed weak and non-significant correlation. On the other hand, our study showed a strong correlation and a high sensitivity of 100%.

Regarding power, our study achieved a high power for all tools in the grading system. Likewise, in the clinical classification all tools achieved a high power, although only AD 3D and AD 2D have a good effect size, respectively large (75%) and medium (62%) effect size.

Nonetheless, both depictions of the lumen had small effect sizes (Table 3.3). Therefore, a study with more OHNS participants would be indicated to increase study effect size for visualization models LU 2D and LU 3D.

The awareness of the 2D and 3D depictions' screening capability associated with the support of OHNS community can lead to a prioritization of the assistance to likely affected patients. In addition, in a scenario where a patient already has a CBCT of the craniofacial structures taken for another reason, OHNS can rely on the CBCT 3D depiction which might eliminate the need for a NE in some cases, for instance non-surgical cases. Therefore, a multidisciplinary cooperation can fast-track referral to and consequently management of affected individuals by an OHNS. Altogether those actions can benefit individual and overall community health, in view of the fact that wait times for specialist consultation and treatment delay may increase the rate of deterioration in general physical conditions, and also can lead to more complex medical interventions.(20)

Considering that the 3D visualization depictions were assessed individually and the examiners were blinded to the other depictions of the same case, we believe that even better results would be achieved if the examiner would have access to the 2 different types of depictions for the same individual, or even had access to the CBCT scans and 3D depiction tools at the same time. Another supposition is that the concomitant use of 2D picture and an IPad with 3D volume reconstruction- allowing motion of the 3D surface- would probably have a good performance as the 3D depiction. Ultimately, our intention for using these visualization tools is to refer all patients with enlarged adenoids for full appropriate assessment, therefore the implementation of history and physical examination would definitely qualify for an enlarged adenoid diagnosis.

3.4. Additional findings

Although it wasn't our objective to investigate a qualitative assessment of the technique, but since we had volume numeric measurement information, we analyzed the proportion of the relationship between LU and AD, and compared them to the reference standard. A previous study(13) analyzed the volumetric reconstruction of the minimal cross-sectional area of the Dolphin with the grading of the NE, and they didn't find any correlation between the measurements. On the contrary, based on the measurements we obtained in our sample, the proportionality of the lumen and the soft tissue seems to be linked to the grading according to Parikh, 2006(42) and Ysunza et al..(109) In this sense, we observed a lumen over 24% - 25% for grade 1 and 2, while in grade 3 and 4, it was between 17% - 20% (figure 3.7 - A).

The adenoid size also showed a greater proportion for the AH (grade 3 and grade 4) cases. Therefore our landmarks and techniques allowing the volume measuring (quantitative measurement) of both lumen and adenoid tissue gives light to a very promising new grading for AH screening through CBCT scans, in which non-enlarged adenoids would have an AD lower than 76%, and enlarged cases would have an AD over 76% (figure 3.7- B). Similarly, but in qualitatively mid-sagittal slice view assessment, Major et al., 2014(15) established a corresponding percentage of <25% for grade 1, 25-50% for grade 2, 50-75% for grade 3 and > 75% for grade 4, which means <75% for non-enlarged, and >75% for enlarged adenoids.

3.5. Limitations

The main limitation was the sample size. We contacted 28 OHNS and residents and only 6 answered the emails and among them 4 declined to participate due to scheduling problems, and 2 accepted to participate.

Another limitation was the reference standard that was used. The models were selected based on the retrospective grading of only one evaluation. Neither inter-rater reliability (agreement) nor intra-rater reliability (consistency) was assessed.

3.6. CONCLUSION

Our finding support the validation of the use of 3D printed model depictions of the adenoid obstruction of the nasopharynx. Accuracy was found in two 3D printed models depictions-LU 3D and AD 3D- and in one 3D picture depiction- AD 2D. Screening capabilities of the four 3D depictions tools are presented below:

- LU 2D visualization tool is reliable between repeated evaluations and has high specificity; however it is not accurate, has low sensitivity, and has poor performance on PPV and NPV;
- AD 2D visualization tool is reliable between repeated evaluations and accurate compared with NE (reference standard). It also has high sensitivity and specificity;
- LU 3D visualization tool is reliable between repeated evaluations and showed moderate accuracy, low sensitivity and specificity;
- AD 3D visualization tool is reliable and accurate for evaluating AH compared with NE (reference standard). This depiction presented the highest sensitivity, and highest values for PPV and NPV compared to the other visualization tools.

3.7. Further steps

1) Use a reference standard (NE based assessment OHNS) supported by adequate inter- and intra-reliability values.
2) Apply the research to OHNS from different countries.
3) Analyze the 3D model development technique using different software.
4) Exploration of the 3D depictions as an educational tool.

3.9. Figures & Tables

Figure 3. 1 - 3D Depictions

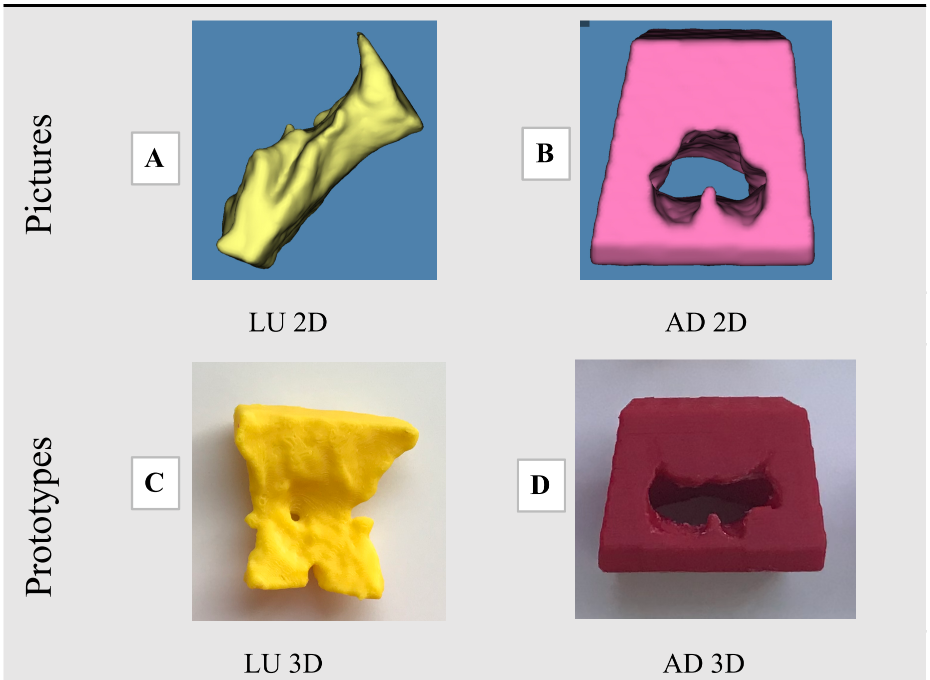

Figure 3. 2 - Sheet A sent to OHNS to grade the 3D Image of airway surface

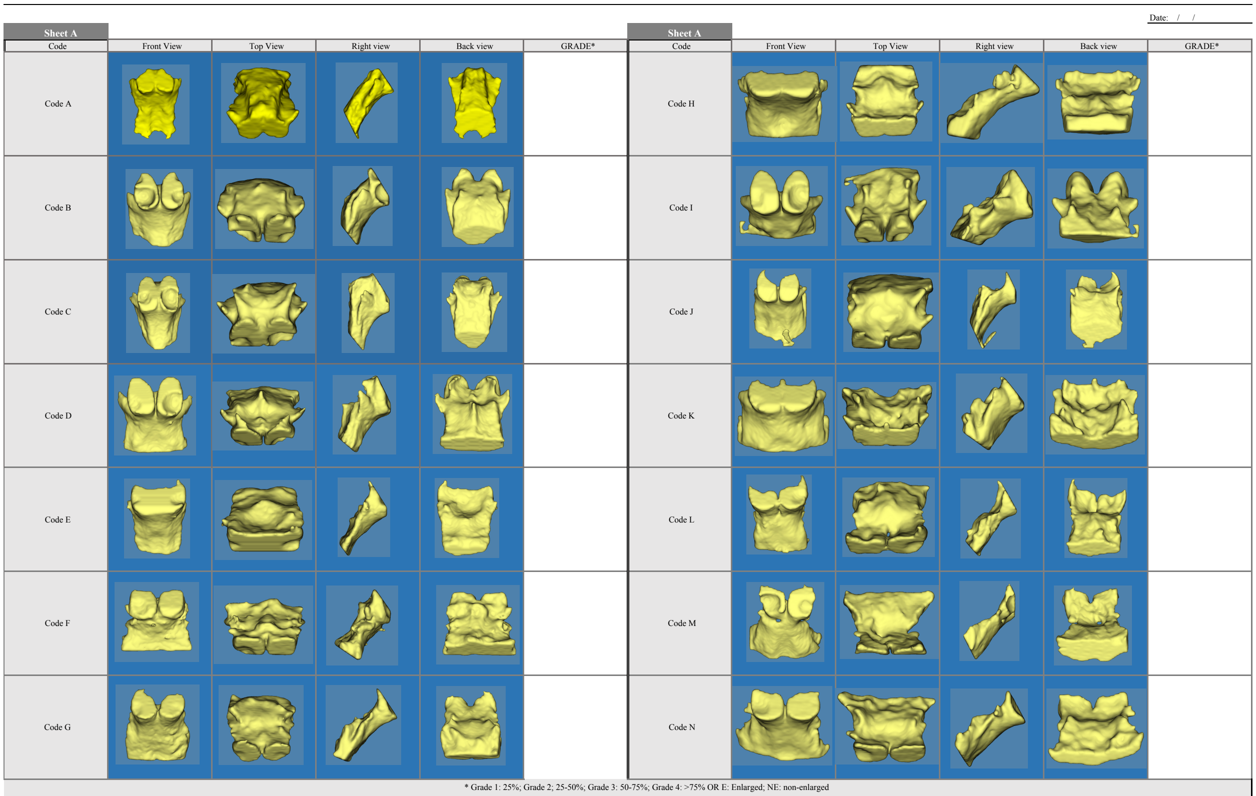

Figure 3. 3- Sheet A1 sent to OHNS to grade the 3D image of the adenoid mass surface

Date: / /

Sheet A1			Sheet A1		
Code	3D Image	GRADE*	Code	3D Image	GRADE*
Code O	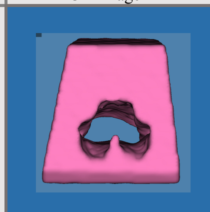		Code V	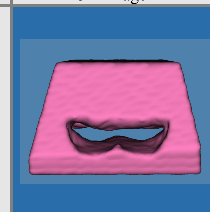	
Code P			Code X	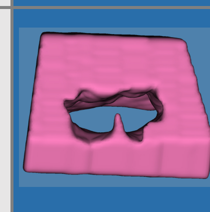	
Code Q	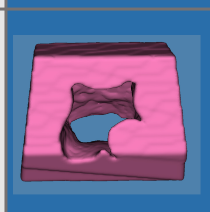		Code W		
Code R			Code Z	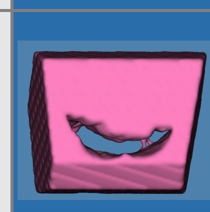	
Code S	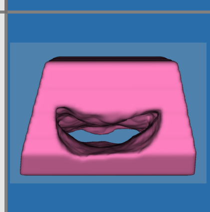		Code AA	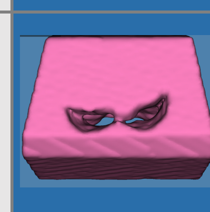	
Code T			Code BB	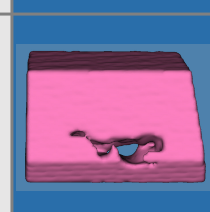	
Code U			Code CC	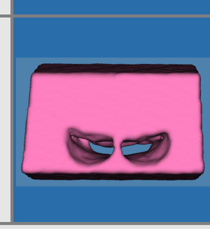	

* Grade 1: 25%; Grade 2; 25-50%; Grade 3: 50-75%; Grade 4: >75% OR E: Enlarged; NE: non-enlarged

Figure 3. 4 - Sheet B sent to OHNS to grade the 3D Image of airway surface

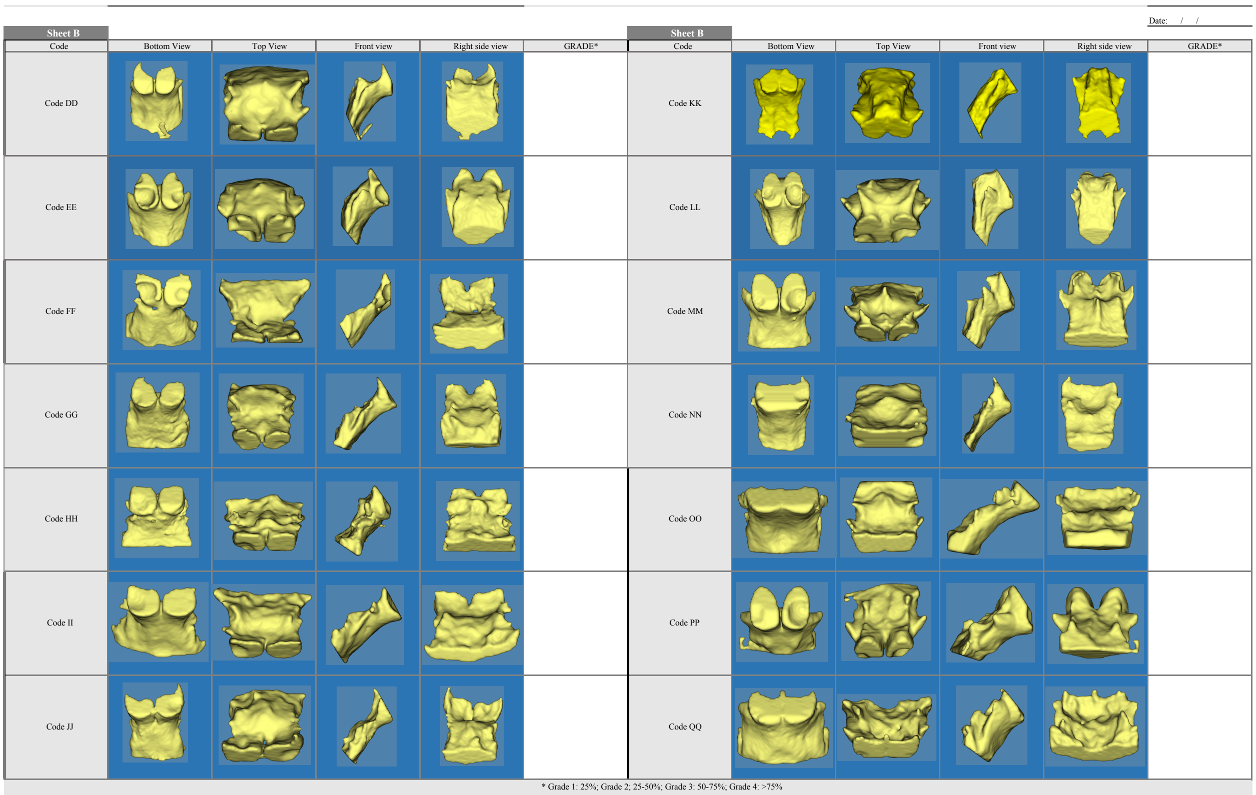

Figure 3. 5 - Sheet B1 send to OHNS to grade the 3D image of the adenoid mass surface

Date: / /

Sheet B1			Sheet B1		
Code	3D Image	GRADE*	Code	3D Image	GRADE*
Code RR	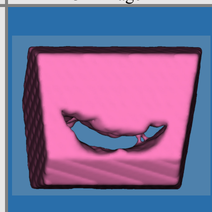		Code YY	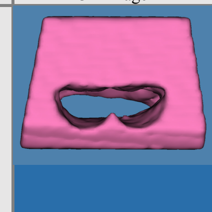	
Code SS	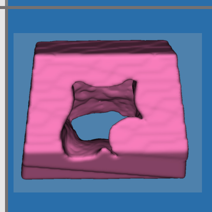		Code ZZ		
Code TT			Code LE	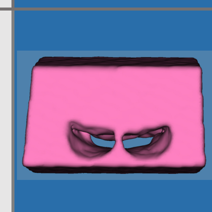	
Code UU	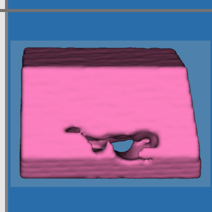		Code PE		
Code VV			Code FE	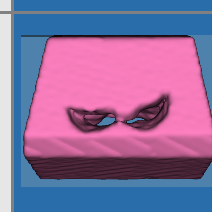	
Code WW			Code MA	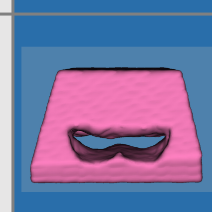	
Code XX	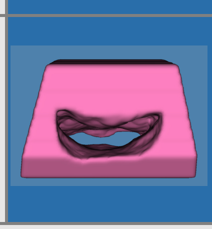		Code AN	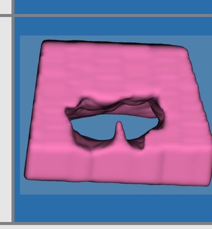	

* Grade 1: 25%; Grade 2; 25-50%; Grade 3: 50-75%; Grade 4: >75% OR E: Enlarged; NE: non-enlarged

Figure 3. 6- 3D printed models (prototypes)

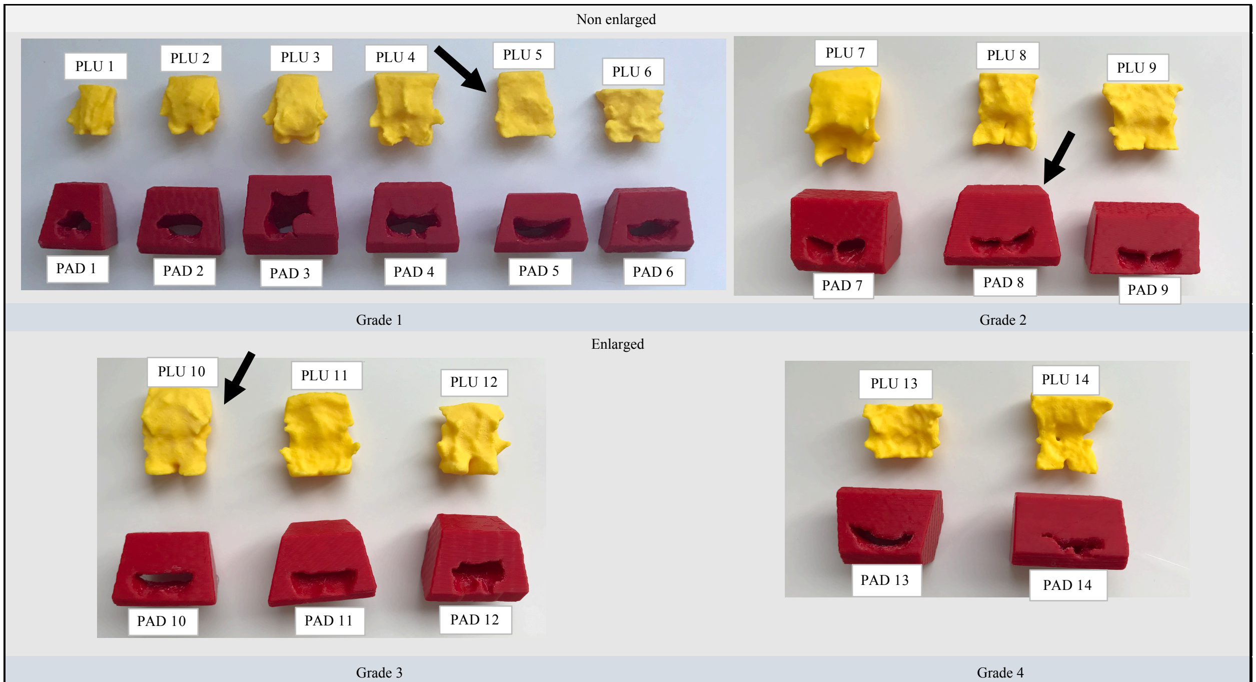

Prototype yellow (LU-lumen); prototype Red (AD-adenoid & soft tissue). Grade 1: 25%; Grade 2: 25-50%; Grade 3: 50-75%; Grade 4: >75%

Figure 3. 7- Volume proportion by Grade and by Category

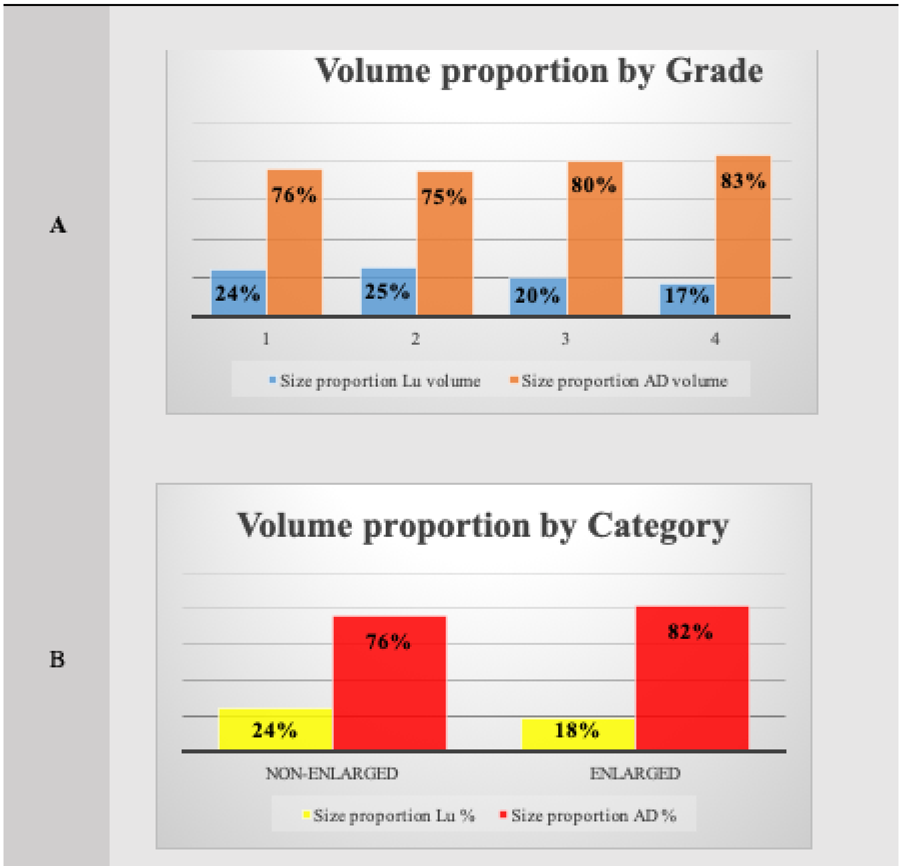

Table 3. 1- Sheet P1 send to OHNS to grade the prototypes (LU)

Date: / /

Sheet P1	Prototype Code	GRADE*	Sheet P1	Prototype Code	GRADE*
LUMEN (LL	PLU1		Adenoid(AD)	PAD1	
	PLU2			PAD2	
	PLU3			PAD3	
	PLU4			PAD4	
	PLU5			PAD5	
	PLU6			PAD6	
	PLU7			PAD7	
	PLU8			PAD8	
	PLU9			PAD9	
	PLU10			PAD10	
	PLU11			PAD11	
	PLU12			PAD12	
	PLU13			PAD13	
	PLU14			PAD14	

* Grade 1: 25%; Grade 2; 25-50%; Grade 3: 50-75%; Grade 4: >75%

Table 3. 2- Sheet P2 send to OHNS to grade the prototypes

				Date: / /	
Sheet P2	Prototype Code	GRADE*	Sheet P2	Prototype Code	GRADE*
LUMEN (LU	PLU15		ADENOID (AD	PAD15	
	PLU16			PAD16	
	PLU17			PAD17	
	PLU18			PAD18	
	PLU19			PAD19	
	PLU20			PAD20	
	PLU21			PAD21	
	PLU22			PAD22	
	PLU23			PAD23	
	PLU24			PAD24	
	PLU25			PAD25	
	PLU26			PAD26	
	PLU27			PAD27	
	PLU28			PAD28	
* Grade 1: 25%; Grade 2; 25-50%; Grade 3: 50-75%; Grade 4: >75%					

Table 3. 3- Statistical Power Analysis

3D depictions	Grading system*		Clinical classification**	
	Observed Power	Effect size	Observed Power	Effect size
LU 2D	1	96%	0.92	53%
AD 2D	1	95%	0.98	62%
LU 3D	1	95%	0.84	47%
AD 3D	1	97%	1	75%

*accordigly to Parikh et al, 2006 (grade 1, 2 3 and 4); **enlarged and non-enlarged

Table 3. 4- Reliability (Inter-reliability, ICC)

	Grading system*		Clinical classification**	
3D depictions	INTER	P-value (95%)	INTER	P-value (95%)
LU 2D	ICC=0.64, CI: 0 - 0.68	NS	ICC=0.26, CI: 0.0 - 0.74	NS
AD 2D	ICC=0.88, CI: 0.64 - 0.96	P<0.001	ICC=0.93, CI:0.78 - 0.98	P<0.001
LU 3D	ICC=0.59, CI: 0 - 0.87	P<0.005	ICC=0.26, CI:0.0 - 0.77	NS
AD 3D	ICC=0.79, CI:0.37 - 0.93	P<0.001	ICC=0.73, CI: 0.14 - 0.91	P<0.005

*accordigly to Parikh et al, 2006 (grade 1, 2 3 and 4); **enlarged and non-enlarged

Table 3. 5- Summary of results

3D depictions	Grading system*	Clinical classification**					
	Accuracy		Correlation	Sensitivity	Specificity	PPV	NPV
LU 2D	moderate	poor	no correlation	33%	78%	22 - 29%	59%
AD 2D	strong	moderate	moderately strong	80%	61%	54%	85%
LU 3D	moderate	moderate	weak	55%	64%	47%	72%
AD 3D	almost perfect	almost perfect	strong	100%	70%	60 - 66%	97%

*accordigly to Parikh et al, 2006 (grade 1, 2 3 and 4); **enlarged and non-enlarged

Chapter 4: Discussion & Conclusion

4.1. OVERALL DISCUSSION

The assessment of the upper airway space, while screening for adenoid hypertrophy in children with SDB, is important in order to support adequate multidisciplinary management. Timely intervention may likely prevent any further major health consequences. These consequences potentially involve obstructive sleep apnea syndrome (OSA)(1, 2), poor grade performance, consumption of more medication and financial burden as a need for more specialist consultations. A higher annual impact in health care costs – calculated as an increase of 215% were observed in affected children when compared to a healthy control.(7)

The consequences of not addressing an health issue may increase the rate of deterioration in general physical conditions and also can lead to more complex medical interventions. 51% of Canadians wait extensively for a medical specialist appointment, and 53% waited too long for selected diagnostic tests.(19) The wait times in Canada for an otolaryngology specialist appointment along with eleven other specialties has been considered the longest in the developed world.(20) Having educated and trained health professionals in screening for SDB would allow them to provide a solid referral to a medical specialist.

During the clinical and oral cavity evaluation dentists can identify some phenotypic characteristics linked to sleep related disorder breathing (SRDB), therefore engaging in an essential responsibility in screening and referring potential patients with an increased risk for OSA. Hence, it is essential that general dental practitioners are educated and trained regarding SDB, so they can work closely with a referral system to the proper specialist for diagnosis and treatment.(91) After all, dentists are responsible for the diagnosis, treatment, and prevention of diseases and disorders of the oral cavity and related structures.(21)

Imaging techniques have been indicated to improve evaluation of abnormalities predisposing to obstructive SDB in children.(1) Dynamic imaging methods would provide better quality, due to pharyngeal obstruction site changes between wakefulness and sleep, between sleep stages, according to body position and patient's age.(115) However, they are overall usually associated with high ionizing radiation, expensive, limited availability, and/or sometimes out of the scope of the dentist.(11) In dentistry imaging of the upper airway space and craniofacial structures has traditionally employed lateral cephalometry radiography, but cephalometry whilst informative and readily available, has the 2D procedure as a limitation. On the other hand, CBCT whilst static, has a lower radiation dose, has the 3D technology and has become available specifically for the dentistry field.(30) Therefore, over the years the interest in CBCT in the dentistry field has exponentially increased since its introduction in the late 1990's.(14)

Five studies(13, 15-17, 27) have explored the use of CBCT imaging to investigate pharyngeal adenoidal obstruction thus far. Four(13, 15-17) contrasted CBCT imaging against NE supported diagnosis assessed qualitatively and one(13) quantitatively. The findings of the three(15-17) qualitatively assessments showed a significant gap of agreement in image interpretation between professionals, and a disagreement between CBCT imaging accuracy compared to a NE reference standard. In the qualitatively assessment of CBCT through volume and minimal cross-sectional area(13), a weak correlation was observed. In summary, it seems that use of CBCT imaging, although promising, is not near enough to be an adequate replacement for NE imaging. The reasons for this are related to the static nature of CBCT imaging, the significant computer skills required and the fact that the patient is not present to interact during the imaging process. In spite of the fact that CBCT was not designed to evaluate soft tissue, its reliability and accuracy for measuring soft tissue depth has been investigated in a forensic study.(44) High intra- and inter-reliability were found, as well as high correlation when compared to physical measurements. The study used two distinct scan protocols, 03 and 04 mm voxels, and 17 mm of FOV for both voxel sizes. Similarly, our study used 0.3 mm voxels as a protocol, although a higher FOV (12 in).

Computer-based 3D volume calculations can be performed more accurately, effectively, and easily with the advent of 3D reconstruction and analysis techniques. The 3D imaging reconstruction tool has been positive for complex medical cases as it significantly improves diagnosis and treatment planning. The use of the digital imaging and communications in medicine (DICOM) format allows the 3D reconstructions of complex airway space and anatomy.(29) Furthermore, 3D printing technology that converts a 2D image to a touchable model enables a more comprehensive view of human anatomical structures, especially complex anatomies. The assessment of a 3D printed model generated from a DICOM as a computational aid for screening for abnormalities and obstruction diagnosis of the upper airway has not been explored.

Our study developed and validated the use of 3D printed models of the nasopharyngeal area of patients with different degrees of adenoidal hypertrophy (AH). It explored CBCT scan reconstructions through Dolphin software as a mechanism to screen for AH in comparison to OHNS direct NE assessment of the area.

Our methodology reliability for the design and development of the 3D depiction tools were analyzed using ICC and both intra- and inter-reliability were high. For UA models an ICC

=0.993 (95% CI:0.981-0.998) and for AD model an ICC =0.944 (95% CI: 0.861-0.982) in single measures, were found. Inter-reliability was considered excellent between raters for both models; LU presented an ICC of 0.982; 95% CI, 0.939-0.995); and AD presented an ICC of 0.995; 95% CI, 0.981-0.998). The measurement error for LU was 1.667mm^3 ± 1.000 mm^3 (SD: 37.27), and for AD was: 139.250mm^3±1.006mm^3 (SD: 98.46). The prototypes were developed using the DICOM data analyzed with commercial software Dolphin 3D.

Our validity study showed a moderate and strong correlation (AD 2D and AD 3D respectively) with the reference standard. On the contrary, a previous study(13) failed to find a strong correlation of the volume and cross-sectional 3D and 2D measurements with a NE reference standard. Similarly, our LU 2D and LU 3D, showed no correlation, and weak and non-significant correlation respectively. Likewise, LU 2D, LU 3D and the Pacheco-Pereira et al., 2017(13) study shared the same type of lumen assessment, although the later assessed it quantitatively and this study assessed it qualitatively. Therefore, a further quantitative assessment of our technique would provide a more objective approach.

Additionally, the Pacheco-Pereira et al. (2017), study(13) performance for sensitivity and specificity were poor (66% and 43% for the volume, and 50% and 46% for the minimal cross-sectional area respectively). In our study similar weak results were found for our LU 2D and LU 3D for sensitivity, 33% and 55% respectively. On the other hand, a better performance in specificity was found for all 4 tools, 78% (LU 2D), 61% (AD 2D), 64% (LU 3D) and 70% (LU 3D), which means that more non-enlarged (true-negative)patients were found. On the contrary, strong performances were reported by Major et al. (2014)(15), with sensitivity of 88 % and specificity of 93%. The Major et al. 2014(15) specificity values were higher than all of our 3D tools. However, their sensitive performance was lower than the sensitivity performance achieved by our AD 3D tool.

The 3D visualization depictions were assessed individually and the examiners were blinded to the other depictions of the same case. We believe that better results would be achieved with an association of our technique with Major et al. 2014(15) technique, which consists basically of examiner access to the CBCT scans. To explain it more clearly, a full access to the CBCT reconstruction associated to the printed model.

Our current reference standard validation scale for NE, Parikh et al. (2006)(42), lacks information regarding sensitivity, specificity, PPV, NPV, false positives, false negatives, and correlation analysis. Therefore, more analysis of the diagnostic capability of our depiction with our reference standard couldn't be performed. Nonetheless, we simulated a quantitative analysis of our technique, based on the relationship between LU and AD as compared to the reference standard. Based on the measurements we obtained in our sample, the proportionality of the LU and AD covering the nasopharynx seems to be linked to the grading according to a four-point (42), and percentage of obstruction(109) scales. In this sense, we observed a lumen over 24% - 25% for grade 1 and 2, while in grade 3 and 4, it was between 17% - 20% (figure 3.7 A).

In addition, the adenoid size also showed a greater proportion for the adenoid hypertrophic (grade 3 and grade 4) cases. Therefore, our landmarks and techniques allowed the volume measurement and the quantitative measurement of both lumen and adenoid tissue. It gives light to a new and potentially useful grading for adenoid hypertrophy screening through CBCT scans. Our speculation, based on our sample findings, is that in this quantitative assessment through CBCT, non-enlarged adenoids patients would have an AD $< 76\%$ (grade 1 and grade 2), and enlarged cases would have an AD $\geq 77\%$ (figure 3.7 B). Similarly, but in qualitatively mid-sagittal slice view assessment, Major et al.(15) used a correspondent percentage of <25% for grade 1, 25-50% for grade 2, 50-75% for grade 3 and > 75% for grade 4, which means <75% for non-enlarged, and >75%, based on a previous reported four-point scale by Ysunza et al..(109) Obviously, a further discriminant analysis would be necessary to better address the supposed proportion for CBCT.

Our methodology to obtain the four 3D depictions of the nasopharyngeal adenoidal obstruction was reliable. We used a new version of Dolphin software in which an inverted threshold can be used, allowing for better delimitation of bone and soft tissue. Dolphin software is user friendly in clinical settings and saves the volume surface directly to the STL file, simplifying the 3D printing process.

Dolphin software has a sensitivity tool to identify the density value in the scan. Although called HU in the software, its value does not correspond to the specific HU value of 0 for water and -1000 for air specific to CT machines. It is also important to recall that HU is not a standardized system, The "HU value" may not be the same if using the same CT machine but with a different technique, as well as if using a different machine.(58) Additionally, variation in scanning parameters affect the measured density values(58) and the HU cut off value can have a major bearing in the volume measurement results as well as on the 3D surface. That is the fundamental reason why the sensitivity threshold tool must be checked, adjusted, standardized and properly reported in upper airway imaging studies. Therefore, caution should be taken regarding standardizing the threshold sensitivity in upper airway imaging studies to avoid unreliable results if any comparisons of the measurements are made without standardizing the threshold sensitivity tool. In the present study, we adjusted the Dolphin threshold to a value of 35

HU for the airway, based on the scan protocol of 6.19 mAs, at 110 kV, FOV 12 in, 0.3 mm voxel, and 8.9-second scan time. A higher HU deformed the surface as seen in figure 2.10.

Our study achieved almost perfect agreement in overall inter-examiner assessment of adenoid size. Between the 2D and 3D depiction types, the 3D showed better results, and comparing the types of view, LU and AD, the “AD'’ type showed better results. We assumed this occurred because the 3D depictions - prototypes- in which the 3D reconstruction allowed touching and looking to real depth of the nasopharyngeal and the adenoid along with its relationship with adjacent structures is possible. For the difference between the types of view LU and AD, we assumed that the best performance of the latter would be due to the familiarity of the examiners with this type of view that is similar to the NE and for the possibility of the view of the relationship between the adenoid and the nasopharynx space availability.

Screening tools and diagnostic tests based on subjectivity evaluation are fallible to some extent, since all humans respond with some inconsistency. That is why on those tests is expected a higher variance among evaluation. Cumulative errors leading to high variability could be associated to evaluators tiredness, and manipulation resulting in evaluation of the wrong side of the prototype.

Overall, the 3D depiction tools showed different diagnostic capabilities. Excellent sensitivity and specificity were observed for the AD 3D (100%, 70%). The AD 3D tool achieved the study goal for correctly identifying enlarged adenoids with only 5% of false-negative cases (Figure 4.1)

Regarding power, our study achieved a high power for all tools in the grading system. Likewise, in the clinical classification all tools achieved a high power, although only AD 3D and AD 2D have a good effect size (large (75%) and medium (62%) effect size respectively).

Nonetheless, a study with more examiners would be indicated to narrow down the errors or variances that would culminate from having multiple opinions.

One noted study limitation is that the HU selection is still a major limitation in the upper airway CBCT imaging field. In our study we used the same threshold (35 HU) for all LU depictions, notice that in a machine and/or under a different scanning protocol the threshold would be different. However, by far our biggest limitation of our study was recruiting participants as only 21.42% (n = 6) answered our invitation, and among them, only 33.33% (n = 2) accepted to participate.

Clinical implications of the study are that the proposed 3D tools may play an essential role in screening for adenoid hypertrophy after more studies in this regard are completed to further validate or not this approach. Specially because CBCT is not an independent exam, as shown in this study, as it is always complemented by a specialist consultation and clinical examination.

Another potential implication of the study is the potential of the 3D depiction tools as an educational tool. Since, they are capable of providing tactile feedback and actual depth information about anatomic and pathologic cases. The same technique with some design adjustments could be applied for different purposes. One example is the development of an algorithm, another would be that the use of the anatomical model for educational purposes for assessing the nasopharynx space by adaptation of the technique and modification of the ROI making its use for basic scope navigation. Therefore, it may be used for undergrad students, dentists, as well as for patients to educate and raise awareness in affected patients and especially their parents about the importance of looking for a specialist.

4.2. CONCLUSION

The present research project aimed to develop and validate 3D depictions of the nasopharyngeal adenoidal area. As suggested in the first Chapter, there is a need for early referral of affected children and CBCT imaging, when available, could help streamline this referral. The 3D depictions seem to be a potential educational tool for further application in the understanding of the nasopharyngeal adenoidal region.

In Chapter 2 we rejected our null hypothesis for the first objective that there is no reliable methodology for the development of 3D depictions of the nasopharyngeal adenoidal area. Our method appears to be reliable to create 3D printed models of the adenoidal area.

In Chapter 3, the null hypotheses that the 3D depiction tools were not accurate was rejected for three out of four 3D depiction tools - AD 2D, LU 2D, and AD 3D, but with different degrees of diagnostic performance.

Overall our study was successful in developing and validating a prototype of the nasopharyngeal adenoidal region using Dolphin software.

4.3. Figures

Figure 4 1– Performance of 3D depictions regarding false-positive and false-negative cases

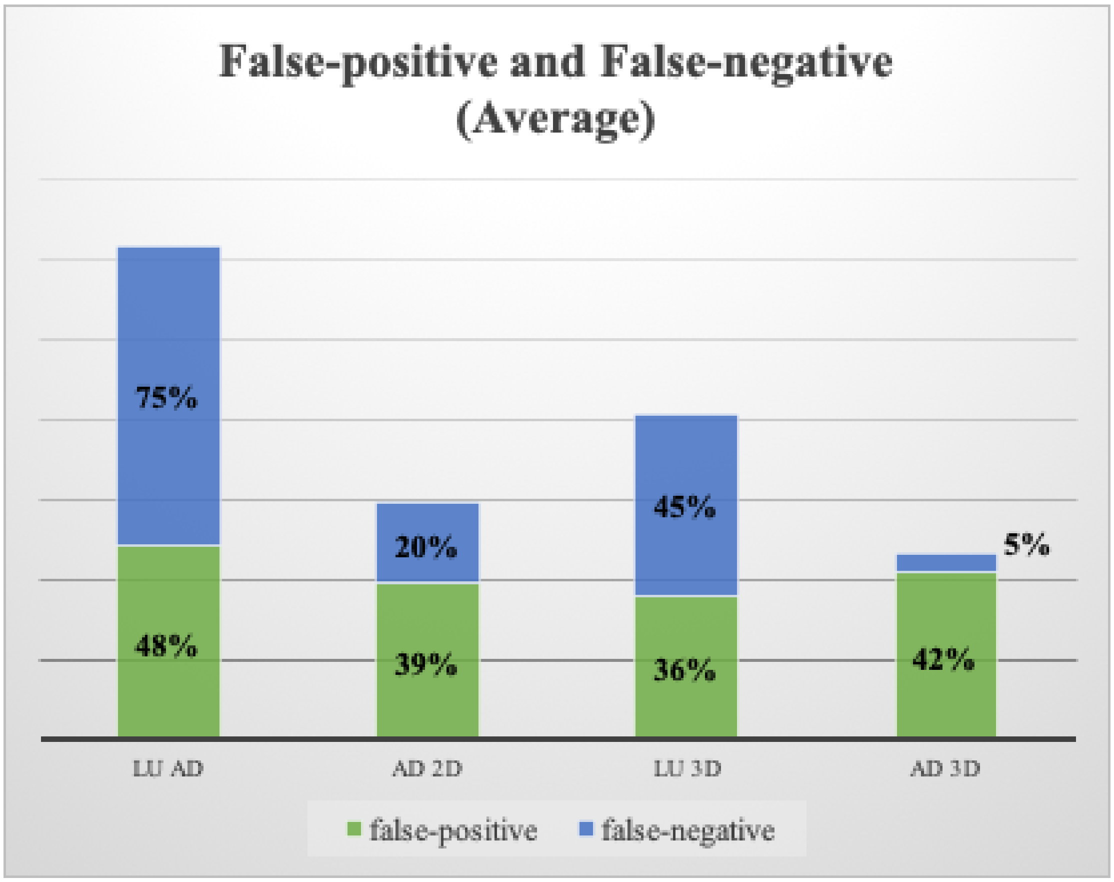

BIBLIOGRAPHY

1. Kaditis AG, Alvarez MLA, Boudewyns A, Alexopoulos EI, Ersu R, Joosten K, et al. Obstructive sleep disordered breathing in 2-to 18-year-old children: diagnosis and management. European Respiratory Journal. 2016;47(1):69-94.

2. Licameli GR TD. Pediatric otorhinolaryngology : diagnosis and treatment. In: Licameli GR, Tunkel DE, editors. 2013.

3. Lumeng JC, Chervin RD. Epidemiology of pediatric obstructive sleep apnea. Proceedings of the American Thoracic Society. 2008;5(2):242-52.

4. Ehsan Z, Ingram DG. Economic and social costs of sleep apnea. Current Pulmonology Reports. 2016;5(2):111-5.

5. Skaer TL, Sclar DA. Economic implications of sleep disorders. Pharmacoeconomics. 2010;28(11):1015-23.

6. Hillman DR, Murphy AS, Antic R, Pezzullo L. The economic cost of sleep disorders. Sleep. 2006;29(3):299-305.

7. Tarasiuk A, Greenberg-Dotan S, Simon-Tuval T, Freidman B, Goldbart AD, Tal A, et al. Elevated morbidity and health care use in children with obstructive sleep apnea syndrome. American journal of respiratory and critical care medicine. 2007;175(1):55-61.

8. Brambilla I, Pusateri A, Pagella F, Caimmi D, Caimmi S, Licari A, et al. Adenoids in children: Advances in immunology, diagnosis, and surgery. Clinical Anatomy. 2014;27(3):346-52.

9. Becking BE, Verweij JP, Kalf-Scholte SM, Valkenburg C, Bakker EW, van Merkesteyn JP. Impact of adenotonsillectomy on the dentofacial development of obstructed children: a systematic review and meta-analysis. European journal of orthodontics. 2017;39(5):509-18.

10. Steen LH. Design and validation of a practical simulator for the development of basic nasal endoscopy skills in otolaryngology – head and neck surgery. University of Alberta; 2015. p. 1-167.

11. Baldassari CM, Choi S. Assessing adenoid hypertrophy in children: X-ray or nasal endoscopy? The Laryngoscope. 2014;124(7):1509-10.

12. Schwab RJ. Upper airway imaging. [Review] [102 refs]. Clinics in Chest Medicine. 1998;19(1):33-54.

13. Pacheco-Pereira C, Alsufyani N, Major M, Palomino-Gomez S, Pereira JR, Flores-Mir C. Correlation and reliability of cone-beam computed tomography nasopharyngeal volumetric and area measurements as determined by commercial software against nasopharyngoscopy-supported diagnosis of adenoid hypertrophy. American Journal of Orthodontics & Dentofacial Orthopedics. 2017;152(1):92-103.

14. Guijarro-Martinez R, Swennen GR. Cone-beam computerized tomography imaging and analysis of the upper airway: a systematic review of the literature. Int J Oral Maxillofac Surg. 2011;40(11):1227-37.

15. Major MP, Witmans M, El-Hakim H, Major PW, Flores-Mir C. Agreement between cone-beam computed tomography and nasoendoscopy evaluations of adenoid hypertrophy. American Journal of Orthodontics and Dentofacial Orthopedics. 2014;146(4):451-9.

16. Pacheco-Pereira C, Alsufyani NA, Major M, Heo G, Flores-Mir C. Accuracy and reliability of orthodontists using cone-beam computerized tomography for assessment of adenoid hypertrophy. American Journal of Orthodontics & Dentofacial Orthopedics. 2016;150(5):782-8.

17. Pacheco-Pereira C, Alsufyani NA, Major MP, Flores-Mir C. Accuracy and reliability of oral maxillofacial radiologists when evaluating cone-beam computed tomography imaging for adenoid hypertrophy screening: a comparison with nasopharyngoscopy. Oral Surgery, Oral Medicine, Oral Pathology and Oral Radiology. 2016;121(6).

18. Fleming J, Al-Radhi Y, Kurian A, Mitchell D. Comparative study of flexible nasoendoscopic and rigid endoscopic examination for patients with upper aerodigestive tract symptoms. The Journal of Laryngology & Otology. 2013;127(10):1012-6.

19. Clarke J. Difficulty accessing health care services in Canada: Statistics Canada Ottawa, Ontario, Canada; 2016.

20. Barua B, Esmail N, Jackson T. The effect of wait times on mortality in Canada: Fraser Institute Vancouver; 2014.

21. Gambhir RS. Primary care in dentistry - an untapped potential. Journal of family medicine and primary care. 2015;4(1):13-8.

22. Code of Ethics [Internet]. 2007 [cited December 31st, 2018].

23. Roopavath UKK, Deepak M. 3D Printing in Medicine. First Edition ed: Elsevier; 2017. p. 1-17.

24. Tokede O, Ramoni RB, Patton M, Da Silva JD, Kalenderian E. Clinical documentation of dental care in an era of electronic health record use. Journal of Evidence Based Dental Practice. 2016;16(3):154-60.

25. Charangowda B. Dental records: An overview. Journal of forensic dental sciences. 2010;2(1):5.

26. Mitsouras D, Liacouras P, Imanzadeh A, Giannopoulos AA, Cai T, Kumamaru KK, et al. Medical 3D printing for the radiologist. Radiographics. 2015;35(7):1965-88.

27. Aboudara C, Nielsen I, Huang JC, Maki K, Miller AJ, Hatcher D. Comparison of airway space with conventional lateral headfilms and 3-dimensional reconstruction from cone-beam computed tomography. American Journal of Orthodontics & Dentofacial Orthopedics. 2009;135(4):468-79.

28. Abramson ZR, Susarla S, Tagoni JR, Kaban L. Three-dimensional computed tomographic analysis of airway anatomy. Journal of Oral Maxillofacial Surgery. 2010;68(2):363-71.

29. Hatcher DC. Cone beam computed tomography: craniofacial and airway analysis. Dental Clinics of North America. 2012;56(2):343-57.

30. Slaats MA, Van Hoorenbeeck K, Van Eyck A, Vos WG, De Backer JW, Boudewyns A, et al. Upper airway imaging in pediatric obstructive sleep apnea syndrome. [Review]. Sleep medicine reviews. 2015;21:59-71.

31. Norton NS. Netter's head and neck anatomy for dentistry. In: Netter FH, editor. third edition ed. Philadelphia, PA: Saunders Elsevier; 2017. p. 425-44.

32. Ruben RJ. The adenoid: Its history and a cautionary tale. The Laryngoscope. 2017;127 Suppl 2:S13-s28.

33. Patel NA, Carlin K, Bernstein JM. Pediatric airway study: Endoscopic grading system for quantifying tonsillar size in comparison to standard adenotonsillar grading systems. American journal of otolaryngology. 2017.

34. Bozzini MF, Di Francesco RC. Managing obstructive sleep apnoea in children: the role of craniofacial morphology. Clinics (Sao Paulo, Brazil). 2016;71(11):664-6.

35. Brockmann PE, Damiani F, Gozal D. Sleep-Disordered Breathing in Adolescents and Younger Adults: A Representative Population-Based Survey in Chile. Chest. 2016;149(4):981-90.

36. Marseglia G, Caimmi D, Pagella F, Matti E, Labó E, Licari A, et al. Adenoids during childhood: the facts. International journal of immunopathology and pharmacology. 2011;24(4_suppl):1-5.

37. Bogin B. Patterns of human growth: Cambridge University Press; 1999.

38. Malina RM, Bouchard C, Bar-Or O. Growth, maturation, and physical activity: Human kinetics; 2004.

39. Papaioannou G, Kambas I, Tsaoussoglou M, Panaghiotopoulou-Gartagani P, Chrousos G, Kaditis AG. Age-dependent changes in the size of adenotonsillar tissue in childhood: implications for sleep-disordered breathing. The Journal of pediatrics. 2013;162(2):269-74. e4.

40. Wang DY, Clement P, Kaufman L, Derde MP. Fiberoptic examination of the nasal cavity and nasopharynx in children. Acta oto-rhino-laryngologica Belgica. 1991;45(3):323-9.

41. Pereira L, Monyror J, Almeida FT, Almeida FR, Guerra E, Flores-Mir C, et al. Prevalence of adenoid hypertrophy: A systematic review and meta-analysis. Sleep medicine reviews. 2018;38:101-12.

42. Parikh SR, Coronel M, Lee JJ, Brown SM. Validation of a new grading system for endoscopic examination of adenoid hypertrophy. Otolaryngology—Head and Neck Surgery. 2006;135(5):684-7.

43. Sher AE, Thorpy MJ, Spielman AJ, Shprintzen RJ, Burack B, Mcgregor PA. Predictive value of müuller maneuver in selection of patients for uvulopalatopharyngoplasty. The Laryngoscope. 1985;95(12):1483-7.

44. Fourie Z, Damstra J, Gerrits PO, Ren Y. Accuracy and reliability of facial soft tissue depth measurements using cone beam computer tomography. Forensic Science International. 2010;199(1):9-14.

45. Apuhan T, Yıldırım YS, Özaslan H. The developmental relation between adenoid tissue and paranasal sinus volumes in 3-dimensional computed tomography assessment. Otolaryngology--Head and Neck Surgery. 2011;144(6):964-71.

46. Fleckenstein P. Anatomy in diagnostic imaging. In: Tranum-Jensen J, Myschetzky PS, editors. Third edition. ed2014.

47. Karatas OH, Toy E. Three-dimensional imaging techniques: A literature review. [Review]. European journal of dentistry. 2014;8(1):132-40.

48. Alsufyani NA, Noga ML, Witmans M, Major PW. Upper airway imaging in sleep-disordered breathing: role of cone-beam computed tomography. Oral Radiology. 2017:1-9.

49. White SC, Pharoah MJ. Oral radiology: principles and interpretation: Elsevier Health Sciences; 2014.

50. Schwab RJ, Gefter WB, Hoffman EA, Gupta KB, Pack AI. Dynamic upper airway imaging during awake respiration in normal subjects and patients with sleep disordered breathing. American Review of Respiratory Disease. 1385;148(5):1385-400.

51. Schwab RJ, Gefter WB, Pack AI, Hoffman EA. Dynamic imaging of the upper airway during respiration in normal subjects. Journal of Applied Physiology. 1993;74(4):1504-14.

52. Iwasaki T, Sato H, Suga H, Takemoto Y, Inada E, Saitoh I, et al. Relationships among nasal resistance, adenoids, tonsils, and tongue posture and maxillofacial form in Class II and Class III children. American Journal of Orthodontics & Dentofacial Orthopedics. 2017;151(5):929-40.

53. Indriksone I, Jakobsone G. The influence of craniofacial morphology on the upper airway dimensions. Angle Orthodontist. 2015;85(5):874-80.

54. Yamashina A, Tanimoto K, Sutthiprapaporn P, Hayakawa Y. The reliability of computed tomography (CT) values and dimensional measurements of the oropharyngeal region using cone beam CT: comparison with multidetector CT. Dentomaxillofacial Radiology. 2008;37(5):245-51.

55. Ludlow JB, Ivanovic M. Comparative dosimetry of dental CBCT devices and 64-slice CT for oral and maxillofacial radiology. Oral Surgery, Oral Medicine, Oral Pathology, Oral Radiology, and Endodontology. 2008;106(1):106-14.

56. Kumar M, Shanavas M, Sidappa A, Kiran M. Cone beam computed tomography-know its secrets. Journal of International Oral Health. 2015;7(2):64.

57. Hounsfield GN. Computerized transverse axial scanning (tomography): Part 1. Description of system. The British journal of radiology. 1973;46(552):1016-22.

58. Molteni R. Prospects and challenges of rendering tissue density in Hounsfield units for cone beam computed tomography. Oral surgery, oral medicine, oral pathology and oral radiology. 2013;116(1):105-19.

59. Razi T, Niknami M, Ghazani FA. Relationship between Hounsfield unit in CT scan and gray scale in CBCT. Journal of dental research, dental clinics, dental prospects. 2014;8(2):107.

60. Oh JH, Choi SP, Wee JH, Park JH. Inter-scanner variability in Hounsfield unit measured by CT of the brain and effect on gray-to-white matter ratio. The American Journal of Emergency Medicine. 2019;37(4):680-4.

61. Pauwels R, Jacobs R, Singer SR, Mupparapu M. CBCT-based bone quality assessment: are Hounsfield units applicable? Dentomaxillofacial Radiology. 2014;44(1):20140238.

62. Lee S, Gantes B, Riggs M, Crigger M. Bone density assessments of dental implant sites: 3. Bone quality evaluation during osteotomy and implant placement. International Journal of Oral & Maxillofacial Implants. 2007;22(2).

63. Hakim SG, Glanz J, Ofer M, Steller D, Sieg P. Correlation of cone beam CT-derived bone density parameters with primary implant stability assessed by peak insertion torque and periotest in the maxilla. Journal of Cranio-Maxillofacial Surgery. 2019;47(3):461-7.

64. Lagravère M, Fang Y, Carey J, Toogood R, Packota GV, Major P. Density conversion factor determined using a cone-beam computed tomography unit NewTom QR-DVT 9000. Dentomaxillofacial Radiology. 2006;35(6):407-9.

65. Mah P, Reeves T, McDavid W. Deriving Hounsfield units using grey levels in cone beam computed tomography. Dentomaxillofacial Radiology. 2010;39(6):323-35.

66. Reeves T, Mah P, McDavid W. Deriving Hounsfield units using grey levels in cone beam CT: a clinical application. Dentomaxillofacial Radiology. 2012;41(6):500-8.

67. Katsumata A, Hirukawa A, Okumura S, Naitoh M, Fujishita M, Ariji E, et al. Effects of image artifacts on gray-value density in limited-volume cone-beam computerized tomography. Oral Surgery, Oral Medicine, Oral Pathology, Oral Radiology, and Endodontology. 2007;104(6):829-36.

68. Attanasio R, Bailey DR. Dental management of sleep disorders: John Wiley & Sons; 2013.

69. Masoud AI, Jackson GW, Carley DW. Sleep and airway assessment: A review for dentists. Cranio. 2017;35(4):206-22.

70. Major MP, Saltaji H, El-Hakim H, Witmans M, Major P, Flores-Mir C. The accuracy of diagnostic tests for adenoid hypertrophy: a systematic review. Journal of the American Dental Association (1939). 2014;145(3):247-54.

71. Ligon SC, Liska R, Stampfl Jr, Gurr M, Mülhaupt R. Polymers for 3D printing and customized additive manufacturing. Chemical reviews. 2017;117(15):10212-90.

72. Zaharia C, Gabor A-G, Gavrilovici A, Stan AT, Idorasi L, Sinescu C, et al. Digital Dentistry—3D Printing Applications. Journal of Interdisciplinary Medicine. 2017;2(1):50-3.

73. Mahamood S, Khader MA, Ali H. Applications of 3-D printing in orthodontics: A Review. Int J Sci Stud. 2016;3:267-70.

74. Ebert LC, Thali MJ, Ross S. Getting in touch—3D printing in forensic imaging. Forensic science international. 2011;211(1-3):e1-e6.

75. Ahn SY, Kim NH, Kim S, Karabucak B, Kim E. Computer-aided Design/Computer-aided Manufacturing-guided Endodontic Surgery: Guided Osteotomy and Apex Localization in a Mandibular Molar with a Thick Buccal Bone Plate. Journal of Endodontics. 2018;44(4):665-70.

76. Reymus M, Fotiadou C, Kessler A, Heck K, Hickel R, Diegritz C. 3D printed replicas for endodontic education. International Endodontic Journal. 2019;52(1):123-30.

77. Van der Meer WJ, Vissink A, Ng YL, Gulabivala K. 3D Computer aided treatment planning in endodontics. Journal of Dentistry. 2016;45:67-72.

78. Yahata Y, Masuda Y, Komabayashi T. Comparison of apical centring ability between incisal-shifted access and traditional lingual access for maxillary anterior teeth. Australian Endodontic Journal: the Journal of the Australian Society of Endodontology. 2017;43(3):123-8.

79. Lin WS, Harris BT, Morton D. Use of CBCT Imaging, Open-Source Modeling Software, and Desktop Stereolithography 3D Printing to Duplicate a Removable Dental Prosthesis-A Proof of Concept. Compendium of Continuing Education in Dentistry. 2017;38(8):e5-e8.

80. Martinez-Seijas P, Diaz-Galvis LA, Hernando J, Leizaola-Cardesa IO, Aguilar-Salvatierra A, Gomez-Moreno G. Polymethyl Methacrylate Custom-Made Prosthesis: A Novel Three-Dimension Printing-Aided Fabrication Technique for Cranial and/or Orbital Reconstruction. Journal of Craniofacial Surgery. 2018;29(5):e438-e40.

81. Murat S, Gurbuz A, Kamburoglu K. Fabrication of obturator prosthesis by fusing CBCT and digital impression data. International Journal of Computerized Dentistry. 2018;21(4):335-44.

82. Nuseir A, Hatamleh MM, Alnazzawi A, Al-Rabab'ah M, Kamel B, Jaradat E. Direct 3D Printing of Flexible Nasal Prosthesis: Optimized Digital Workflow from Scan to Fit. Journal of Prosthodontics. 2018;20:20.

83. Verweij JP, Anssari Moin D, Wismeijer D, van Merkesteyn JPR. Replacing Heavily Damaged Teeth by Third Molar Autotransplantation With the Use of Cone-Beam Computed

Tomography and Rapid Prototyping. Journal of Oral & Maxillofacial Surgery. 2017;75(9):1809-16.

84. De Souza N, Kamat S, Chalakkal P, Khandeparker RV. Use of 3D printed model as an aid in surgical removal of a rare occurrence of a compound odontome in the anterior mandible associated with impacted teeth. Journal of Clinical & Experimental Dentistry. 2018;10(7):e721-e5.

85. Ma B, Park T, Chun I, Yun K. The accuracy of a 3D printing surgical guide determined by CBCT and model analysis. The Journal of Advanced Prosthodontics. 2018;10(4):279-85.

86. Reymus M, Fotiadou C, Hickel R, Diegritz C. 3D-printed model for hands-on training in dental traumatology. International Endodontic Journal. 2018;51(11):1313-9.

87. Ye S, Zhao S, Wang W, Jiang Q, Yang X. A novel method for periapical microsurgery with the aid of 3D technology: a case report. BMC Oral Health. 2018;18(1):10.

88. Wang YT, Yu JH, Lo LJ, Hsu PH, Lin CL. Developing Customized Dental Miniscrew Surgical Template from Thermoplastic Polymer Material Using Image Superimposition, CAD System, and 3D Printing. BioMed Research International. 2017;1906197.

89. Alves Jr M, Baratieri C, Mattos CT, Brunetto D, da Cunha Fontes R, Santos JRL, et al. Is the airway volume being correctly analyzed? American Journal of Orthodontics and Dentofacial Orthopedics. 2012;141(5):657-61.

90. Chen H, van Eijnatten M, Aarab G, Forouzanfar T, de Lange J, van der Stelt P, et al. Accuracy of MDCT and CBCT in three-dimensional evaluation of the oropharynx morphology. European journal of orthodontics. 2018;40(1):58-64.

91. Smith HA, Smith ML. The Role of Dentists and primary Care physicians in the Care of patients with Sleep-Related Breathing Disorders. Frontiers in public health. 2017;5:137.

92. Ramakrishna S, Ingle V, Patel S, Bhat P, Dada J, Shah FA, et al. Reversible cardio-pulmonary changes due to adeno-tonsilar hypertrophy. International journal of pediatric otorhinolaryngology. 2000;55(3):203-6.

93. Koca CF, Erdem T, Bayındır T. The effect of adenoid hypertrophy on maxillofacial development: an objective photographic analysis. Journal of Otolaryngology-Head & Neck Surgery. 2016;45(1):48.

94. Gottlieb DJ, Chase C, Vezina RM, Heeren TC, Corwin MJ, Auerbach SH, et al. Sleep-disordered breathing symptoms are associated with poorer cognitive function in 5-year-old children. The Journal of pediatrics. 2004;145(4):458-64.

95. Rhodes SK, Shimoda KC, Waid LR, O'Neil PM, Oexmann MJ, Collop NA, et al. Neurocognitive deficits in morbidly obese children with obstructive sleep apnea. The Journal of pediatrics. 1995;127(5):741-4.

96. Mouradian WE, Berg JH, Somerman MJ. Addressing disparities through dental-medical collaborations, part 1. The role of cultural competency in health disparities: training of

primary care medical practitioners in children's oral health. Journal of Dental Education. 2003;67(8):860-8.

97. Di Carlo G, Polimeni A, Melsen B, Cattaneo PM. The relationship between upper airways and craniofacial morphology studied in 3D. A CBCT study. Orthod Craniofac Res. 2015;18(1):1-11.

98. Guilleminault C, Akhtar F. Pediatric sleep-disordered breathing: New evidence on its development. Sleep medicine reviews. 2015;24:46-56.

99. Brockmann PE, Bertrand P, Castro-Rodriguez JA. Influence of asthma on sleep disordered breathing in children: a systematic review. Sleep Medicine Review. 2014;18(5):393-7.

100. Sharifkashani S, Dabirmoghaddam P, Kheirkhah M, Hosseinzadehnik R. A new clinical scoring system for adenoid hypertrophy in children. Iranian journal of otorhinolaryngology. 2015;27(78):55.

101. Caylakli F, Hizal E, Yilmaz I, Yilmazer C. Correlation between adenoid-nasopharynx ratio and endoscopic examination of adenoid hypertrophy: a blind, prospective clinical study. Int J Pediatr Otorhinolaryngol. 2009;73(11):1532-5.

102. Feres MF, Hermann JS, Cappellette M, Jr., Pignatari SS. Lateral X-ray view of the skull for the diagnosis of adenoid hypertrophy: a systematic review. Int J Pediatr Otorhinolaryngol. 2011;75(1):1-11.

103. Chisholm E, Lew-Gor S, Hajioff D, Caulfield H. Adenoid size assessment: a comparison of palpation, nasendoscopy and mirror examination. Clinical otolaryngology: official journal of ENT-UK; official journal of Netherlands Society for Oto-Rhino-Laryngology & Cervico-Facial Surgery. 2005;30(1):39-41.

104. Zalzal HG, Carr M, Kohler W, Coutras SW. Adenoid Size by Drug Induced Sleep Endoscopy Compared to Nasopharyngeal Mirror Exam. International Journal of Pediatric Otorhinolaryngology. 2018.

105. Kubba H, Bingham BJ. Endoscopy in the assessment of children with nasal obstruction. The Journal of Laryngology & Otology. 2001;115(5):380-4.

106. Lertsburapa K, Schroeder Jr JW, Sullivan C. Assessment of adenoid size: A comparison of lateral radiographic measurements, radiologist assessment, and nasal endoscopy. International journal of pediatric otorhinolaryngology. 2010;74(11):1281-5.

107. Saedi B, Sadeghi M, Mojtahed M, Mahboubi H. Diagnostic efficacy of different methods in the assessment of adenoid hypertrophy. American journal of otolaryngology. 2011;32(2):147-51.

108. Thereza-Bussolaro CO, Hee So; Lagravère, M; Flores-Mir, C. Pharyngeal Dimensional changes in Class II malocclusion treatment when using Forsus® or intermaxillary elastics - An Exploratory Study. International Orthodontics. 2019;4th (December).

109. Ysunza A, Pamplona MC, Ortega JM, Prado H. Video fluoroscopy for evaluating adenoid hypertrophy in children. Int J Pediatr Otorhinolaryngol. 2008;72(8):1159-65.

110. Weissheimer A, de Menezes LM, Sameshima GT, Enciso R, Pham J, Grauer D. Imaging software accuracy for 3-dimensional analysis of the upper airway. American Journal of Orthodontics and Dentofacial Orthopedics. 2012;142(6):801-13.

111. Modrzynski M, Zawisza E. The influence of birch pollination on the adenoid size in children with intermittent allergic rhinitis. International journal of pediatric otorhinolaryngology. 2007;71(7):1017-23.

112. Valerie R, Saridin JK, Bouw F, Murawska MM, Koudstaal MJ. Measuring upper airway volume: accuracy and reliability of Dolphin 3D software compared to manual segmentation in craniosynostosis patients. Journal of Oral and Maxillofacial Surgery. 2014;72(1):139-44.

113. Pinheiro ML, Yatabe M, Ioshida M, Orlandi L, Dumast P, Trindade-Suedam IK. Volumetric reconstruction and determination of minimum crosssectional area of the pharynx in patients with cleft lip and palate: comparison between two different softwares. Journal of Applied Oral Science. 2018;26:04.

114. Guijarro-Martinez R, Swennen GR. Three-dimensional cone beam computed tomography definition of the anatomical subregions of the upper airway: a validation study. Int J Oral Maxillofac Surg. 2013;42(9):1140-9.

115. Shi H, Scarfe WC, Farman AG. Upper airway segmentation and dimensions estimation from cone-beam CT image datasets. International Journal of Computer Assisted Radiology and Surgery. 2006;1(3):177-86.

116. Deutsch ES. Tonsillectomy and adenoidectomy: changing indications. Pediatric clinics of North America. 1996;43(6):1319-38.

117. Fujioka M, Young LW, Girdany B. Radiographic evaluation of adenoidal size in children: adenoidal-nasopharyngeal ratio. American Journal of Roentgenology. 1979;133(3):401-4.

118. Elwany S. The adenoidal-nasopharyngeal ratio (AN ratio): its validity in selecting children for adenoidectomy. The Journal of Laryngology & Otology. 1987;101(6):569-73.

119. WANG DY, Bernheim N, Kaufman L, Clement P. Assessment of adenoid size in children by fibreoptic examination. Clinical Otolaryngology & Allied Sciences. 1997;22(2):172-7.

120. Kurien M, Lepcha A, Mathew J, Ali A, Jeyaseelan L. X-rays in the evaluation of adenoid hypertrophy: It's role in the endoscopic era. Indian Journal of Otolaryngology and Head and Neck Surgery. 2005;57(1):45-7.

121. Kindermann CA, Roithmann R, Lubianca Neto JF. Sensitivity and specificity of nasal flexible fiberoptic endoscopy in the diagnosis of adenoid hypertrophy in children. Int J Pediatr Otorhinolaryngol. 2008;72(1):63-7.

122. Watkins MP, Portney L. Foundations of clinical research: applications to practice: Pearson/Prentice Hall Upper Saddle River, NJ; 2009.

123. Wang D, Clement P, Kaufman L, Derde MP. Fiberoptic evaluation of the nasal and nasopharyngeal anatomy in children with snoring. The Journal of otolaryngology. 1994;23(1):57-60.

124. Mlynarek A, Tewfik MA, Hagr A, Manoukian JJ, Schloss MD, Tewfik TL, et al. Lateral neck radiography versus direct video rhinoscopy in assessing adenoid size. Journal of otolaryngology. 2004;33(6):360-5.

125. Cho J-H, Lee D-H, Lee N-S, Won Y-s, Yoon H-r, Suh B-d. Size assessment of adenoid and nasopharyngeal airway by acoustic rhinometry in children. The Journal of Laryngology & Otology. 1999;113(10):899-905.

126. Wormald P, Prescott C. Adenoids: comparison of radiological assessment methods with clinical and endoscopic findings. The Journal of Laryngology & Otology. 1992;106(4):342-4.

127. Barbosa MdC. Avaliação da rdiografia cefalométrica lateral como meio de diagnóstico da hipertrofia de adenóide. 2005.

Appendices

Appendix A: Research Sample Reasoning & Study Design flowchart

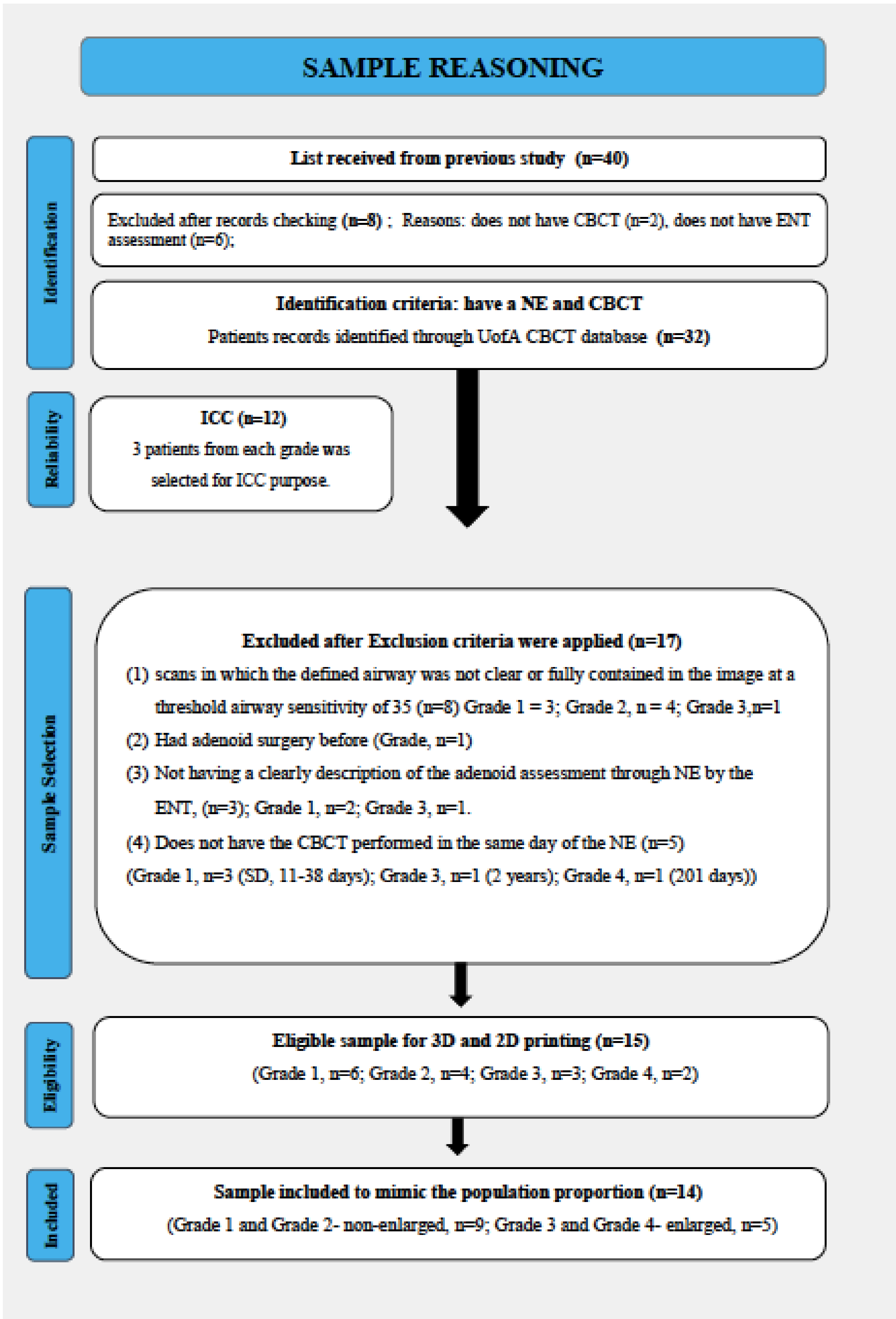

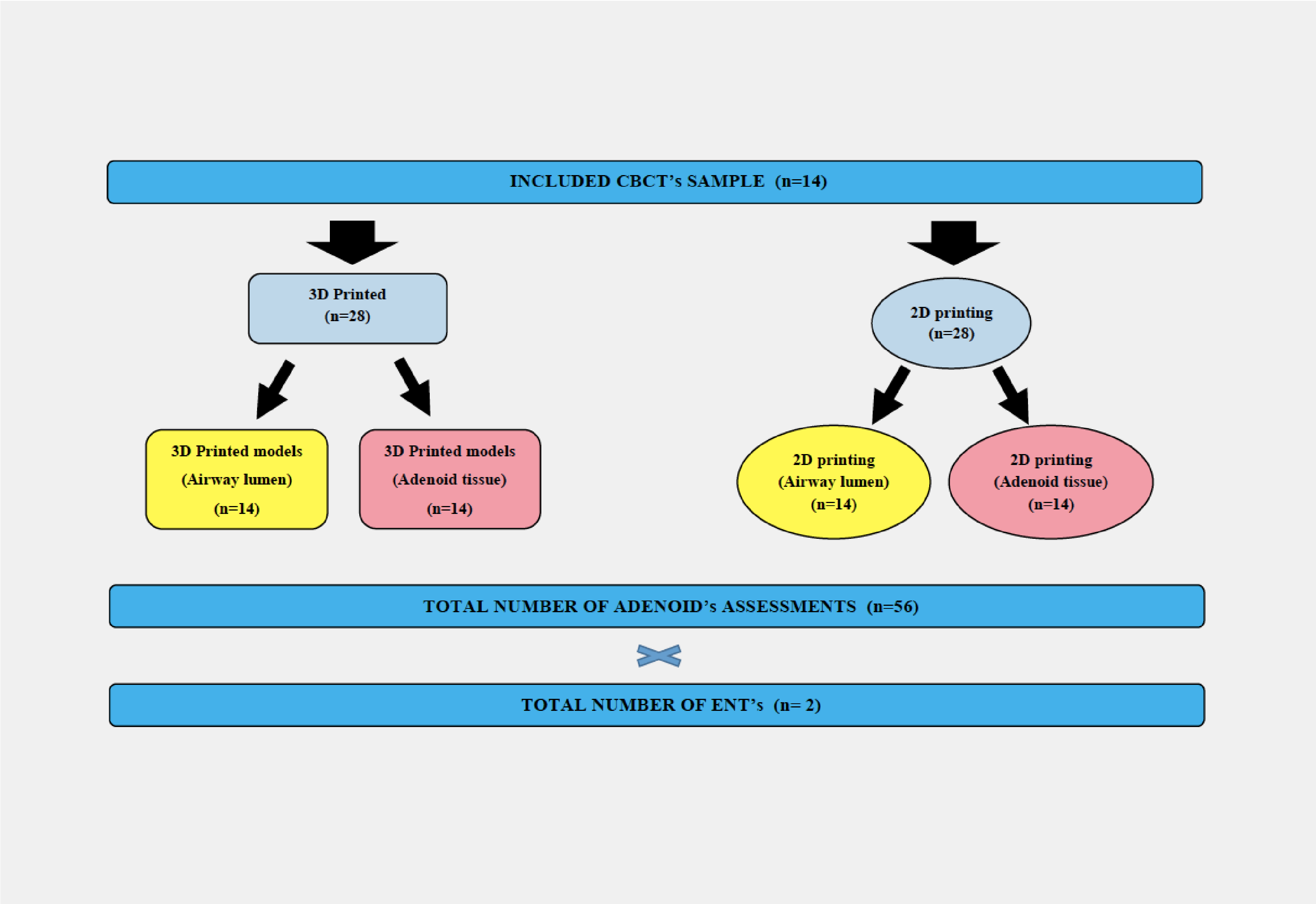
INCLUDED CBCT's SAMPLE (n=14)
3D Printed (n=28)
2D printing (n=28)
3D Printed models (Airway lumen) (n=14)
3D Printed models (Adenoid tissue) (n=14)
2D printing (Airway lumen) (n=14)
2D printing (Adenoid tissue) (n=14)
TOTAL NUMBER OF ADENOID's ASSESSMENTS (n=56)
TOTAL NUMBER OF ENT's (n= 2)

Appendix B: Ethics Approval Hero Pro00082445

Approval Form

Date:	June 19, 2018
Study ID:	Pro00082445
Principal Investigator:	Carlos Flores Mir
Study Title:	Development, Validation, and Application of a 3D reconstruction of Pharyngeal Adenoidal Obstruction Level through Cone Beam Computed Tomography
Approval Expiry Date:	Tuesday, June 18, 2019

Thank you for submitting the above study to the Health Research Ethics Board - Health Panel. Your application, including the following, has been reviewed and approved on behalf of the committee;

- AH Project Proposal (6/11/2018)
- Variables AH Project (5/17/2018)

The Health Research Ethics Board assessed all matters required by section 50(1)(a) of the Health Information Act. It has been determined that the research described in the ethics application is a retrospective chart review for which subject consent for access to personally identifiable health information would not be reasonable, feasible or practical. Subject consent therefore is not required for access to personally identifiable health information described in the ethics application.

In order to comply with the Health Information Act, a copy of the approval form is being sent to the Office of the Information and Privacy Commissioner.

A renewal report must be submitted next year prior to the expiry of this approval if your study still requires ethics approval. If you do not renew on or before the renewal expiry date (Tuesday, June 18, 2019), you will have to re-submit an ethics application.

Approval by the Health Research Ethics Board does not encompass authorization to access the patients, staff or resources of Alberta Health Services or other local health care institutions for the purposes of the research. Enquiries regarding Alberta Health approvals should be directed to (780) 407-6041. Enquiries regarding Covenant Health approvals should be directed to (780) 735-2274.

Sincerely,

Anthony S. Joyce, PhD.
Chair, Health Research Ethics Board - Health Panel

Note: This correspondence includes an electronic signature (validation and approval via an online system).

UNIVERSITY OF ALBERTA   Alberta Health Services   Covenant Health

Appendix C: Invitation Letter

Appendix C: Invitation Letter

Study Information

UNIVERSITY OF ALBERTA

Dear Potential Participant:

As a pediatric otolaryngologist (OHRS) specialist established in Edmonton, I'm contacting you to assess your willingness to participate in a proposed study. You are been asked to take part in a research designed to assess a 3D printed model of the nasopharynx produced from CBCT imaging. More specifically our research question is:

Validation of the use of a 3D printed model depicting Adenoid Hypertrophy in comparisons to a Nasoendoscopy-based grading assessment.

The material consist of a number of twenty-eight (n=28) 3D printed model, representing different degrees of Adenoidal obstruction grade classification according with Parikh SR proposal (2006)

Please take a moment to read the following information:

1) Your participation is voluntary
2) You will be asked to grade a number of 28 generated printed models as representation of nasopharynx airway space 2 times with a week time in between
3) Your responses will remain anonymous and interpretation documents will not contain personal identifiers.
4) This study has received ethical approval from the HERB-Health Panel the University of Alberta, Edmonton, Canada.
5) Once you have submitted the interpretation documents, they will become property of the University of Alberta and cannot be returned to you due to lack of personal identifiers on it.

Thank you for your consideration. If you have any questions or require additional information please contact either my supervisor or myself by the following means should you choose to participate or if you have any questions or concerns (email: bussolar@ualberta.ca or cf1@ualberta.ca). Further information will be provided if you choose to participate.

Sincerely,

Claudine Thereza-Bussolaro
DDS-MSc Candidate (University of Alberta)
Graduate Student – Investigator
(587) 936-2950

Appendix D: Informed consent

UNIVERSITY OF ALBERTA

CONSENT TO PARTICIPATE IN RESEARCH

Validation of the use of a 3D printed model depicting Adenoid Hypertrophy in comparisons to a Nasoendoscopy-based grading assessment.

You are asked to participate in this study because you are a pediatric ENT specialist practicing in Edmonton, AB, Canada. Your participation in this study is entirely voluntary. You should carefully read the information below, and ask questions about anything you do not understand before deciding whether or not to participate.

Purpose of Study & Research Question
Research question: : Is obstruction grading of hypertrophic adenoidal tissue similar when comparing a CBCT-based 3D printed model vs image of CBCT-based 3D surface?
Procedures:
If you volunteer to participate in this study, these procedures will be involved:

- You will review two times a series of 8 3D printed models(prototypes) of the nasopharyngeal area in your office.
- You will review two times a series of 8 3D surface pictures of the nasopharyngeal area in your office.
- you will be asked to report only on your impression about how much adenoid hypertrophy may be clinically relevant
- your reports will be blinded, non-identified, and received on a sealed box/envelope

Privacy and Confidentiality:
No personal information about you, or provided by you during this research, will be disclosed to others. When/if the results of the research are published or discussed in conference, no information will be included that would reveal your identity. Collected data will only be used for this thesis project. Collected information will be stored in an encrypted and password protected computer. Data will be stored for a time of 5 years.
Direct Benefit or Risk of Participation
Involvement will not directly benefit participants, but the findings will help us gain improved insight into the potential use of CBCT imaging, when available for other reasons, as a tool for Adenoid Hypertrophy screening. No risks of participation are expected.
Participation and Withdrawal
You participation in this research is entirely VOLUNTARY. If you choose not to participate, that will not affect your relationship with the University of Alberta. If you decide to participate, you are free to withdraw your consent and discontinue participation at any time without prejudice. If you have any questions or concerns regarding your rights as a research subject, you may contact the University of Alberta's Research ethics office at (780) 492-2615.

Identification of the Investigators:
If you have any questions about the research, please contact any of the investigators listed below:
Project supervisor: Dr. Carlos Flores-Mir……………………cf1@ualberta.ca

Master's student: Claudine Thereza-Bussolaro……………..bussolar@ualberta.ca

Department of Dentistry

ECHA, 5th Floor, 11405- 87 Ave NW • University of Alberta • Edmonton • Canada • T6G 1C9
Telephone: (780) 492-8041 • Fax: (780) 492-1624

Title: Development, Validation, and Application of a 3D Reconstruction of the Nasopharyngeal area to Measure Nasopharynx Obstruction in Cone Beam Computed Tomography in Children

Principal investigator: Claudine Thereza-Bussolaro
Phone number(s): (587) 936-2950

	Yes	No
Do you understand that you have been asked to be in a research study ?	☐	☐
Have you read and received a copy of the attached Information Sheet ?	☐	☐
Do you understand the benefits and risks involved in taking part in this research study ?	☐	☐
Have you had an opportunity to ask questions and/or discuss this study ?	☐	☐
Do you understand that you are free to withdraw from the study at any time. Without having to give a reason ?	☐	☐
Has the issue of confidentiality been explained to you ?	☐	☐

How was this study explained to you ________________________________
____
____

	Yes	No
I agree to take part in this study:	☐	☐

Signature of Participant______________________________________
(Printed Name) ______________________________________
I believe that the person signing this form understands what is involved in the study and voluntarily agrees to participate.

Signature of Investigator or Designee ________________ Date ___/___/______

The information sheet must be attached to this consent form and a copy given to the research subject

Department of Dentistry

ECHA, 5th Floor, 11405- 87 Ave NW • University of Alberta • Edmonton • Canada • T6G 1C9
Telephone: (780) 492-8041 • Fax: (780) 492-1624

Appendix E: Guidance Sheet

Guidance to the ENT:
We made 3D printed models from the volume obtained from the measurement of the nasopharynx space where the Adenoid is located.
As bellow:

Step 1: delimitation of the region of interest (ROI)

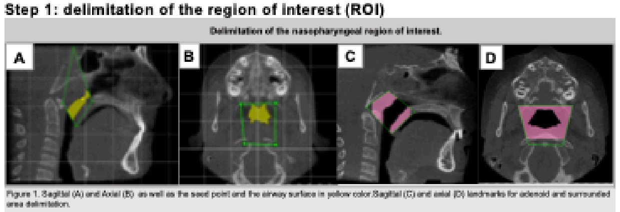

Step 2: generation of the 3D surface files (figure 2 and 3)

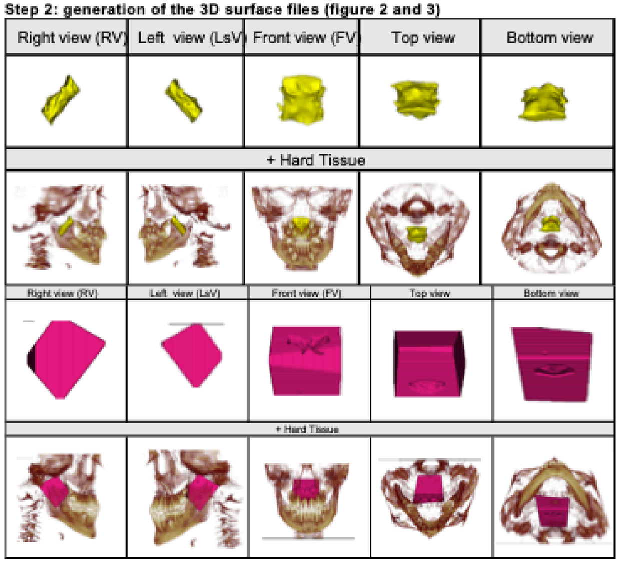

Figure 2: 3D Surfaces representation on hard tissue

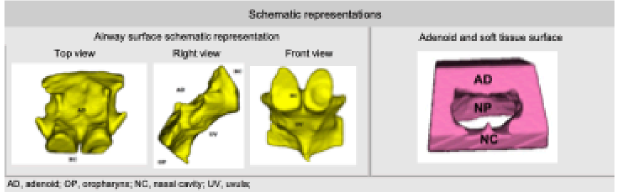

Figure 3: Schematic representation of the 3D surfaces

Step 3: prototype manufacturing:
The surface files were taken to a 3D printed machine and the 3D printed models (Prototypes) were manufactured (Figure below):

Figure 4: Picture of the actual printed models (prototypes, representing grade 1,2,3,and 4 of adenoid hypertrophy.

Appendix F: Information Sheet (Cheat Sheet)

Fig 1F. Nasopharynx obstruction Due to Adenoid tissue Hypertrophy –Grade system for Endoscopic Examination[42]

Table 1
Proposed adenoid staging system: anatomic relationship between the adenoid tissue and vomer, soft palate, and torus tubaris (Eustachian tube orifice)

Grade	Anatomic structures in contact with adenoid tissue
Grade 1	None
Grade 2	Torus tubaris
Grade 3	Torus tubaris Vomer
Grade 4	Torus tubaris Vomer Soft palate (at rest)

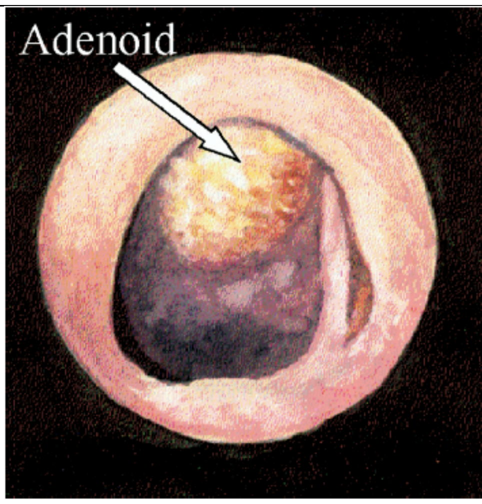

Figure 1 Grade 1, adenoid tissue not in contact with adjacent structures.

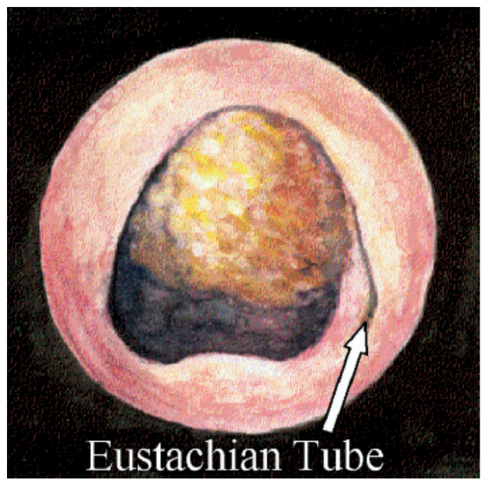

Figure 2 Grade 2, adenoid tissue in contact with torus tubaris.

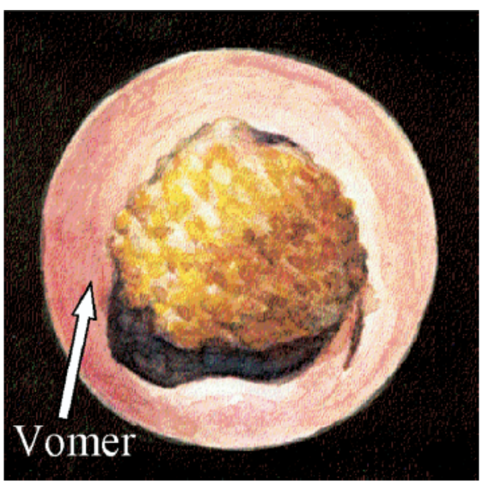

Figure 3 Grade 3, adenoid tissue in contact with Vomer.

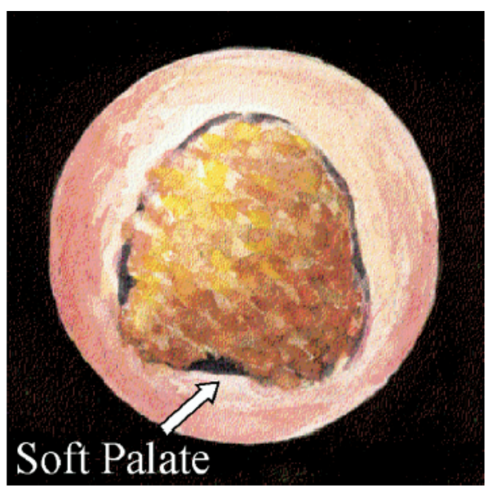

Figure 4 Grade 4, adenoid tissue in contact with palate (at rest).

Correspondent Grade System used for evaluation of CBCT –Mid-sagittal slice [15, 109]

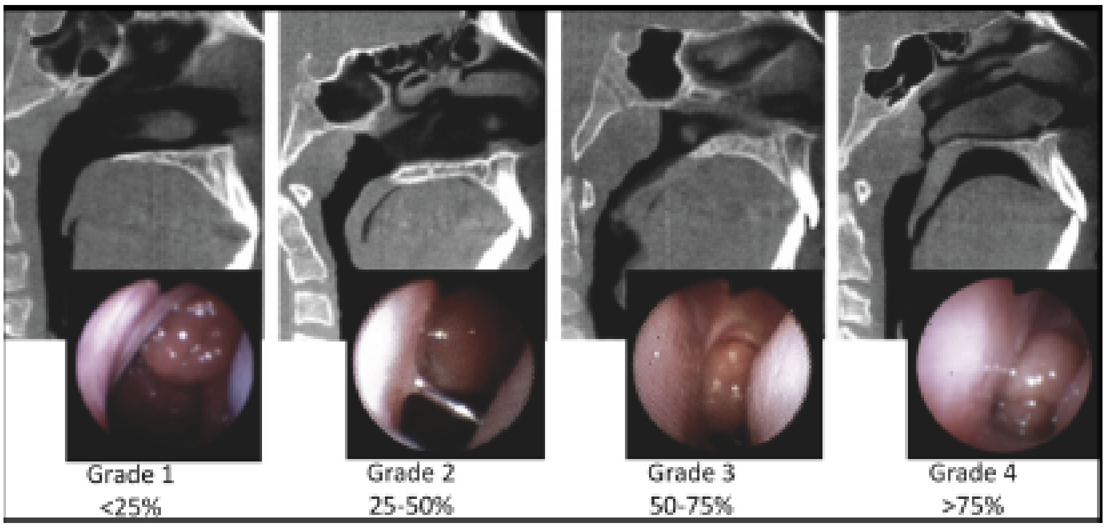

Fig 2F. Adenoid size in CBCT midsagittal slice and corresponding viewed with NE.